



저작자표시-비영리-변경금지 2.0 대한민국

이용자는 아래의 조건을 따르는 경우에 한하여 자유롭게

- 이 저작물을 복제, 배포, 전송, 전시, 공연 및 방송할 수 있습니다.

다음과 같은 조건을 따라야 합니다:



저작자표시. 귀하는 원저작자를 표시하여야 합니다.



비영리. 귀하는 이 저작물을 영리 목적으로 이용할 수 없습니다.



변경금지. 귀하는 이 저작물을 개작, 변형 또는 가공할 수 없습니다.

- 귀하는, 이 저작물의 재이용이나 배포의 경우, 이 저작물에 적용된 이용허락조건을 명확하게 나타내어야 합니다.
- 저작권자로부터 별도의 허가를 받으면 이러한 조건들은 적용되지 않습니다.

저작권법에 따른 이용자의 권리는 위의 내용에 의하여 영향을 받지 않습니다.

이것은 [이용허락규약\(Legal Code\)](#)을 이해하기 쉽게 요약한 것입니다.

[Disclaimer](#)

Master's Thesis

PHYSICAL AND CHEMICAL MODIFICATION
OF POLYMER TO IMPROVE
HYDROPHOBICITY IN MEMBRANE
DISTILLATION

Hyung Kae Lee

Department of Urban and Environmental Engineering
(Environmental Science and Engineering)

Graduate School of UNIST

2017

PHYSICAL AND CHEMICAL MODIFICATION
OF POLYMER TO IMPROVE
HYDROPHOBICITY IN MEMBRANE
DISTILLATION

Hyung Kae Lee

Department of Urban and Environmental Engineering
(Environmental Science and Engineering)

Graduate School of UNIST

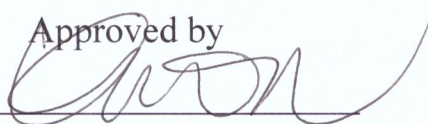
PHYSICAL AND CHEMICAL MODIFICATION
OF POLYMER TO IMPROVE
HYDROPHOBICITY IN MEMBRANE
DISTILLATION

A thesis
submitted to the Graduate School of UNIST
in partial fulfillment of the
requirements for the degree of
Master of Science

Hyung Kae Lee

01. 11. 2017

Approved by



Advisor

Young-Nam Kwon

PHYSICAL AND CHEMICAL MODIFICATION
OF POLYMER TO IMPROVE
HYDROPHOBICITY IN MEMBRANE
DISTILLATION

Hyung Kae Lee

This certifies that the thesis of Hyung Kae Lee
is approved.

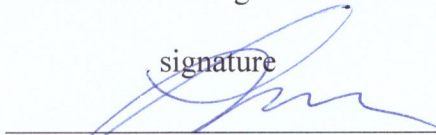
1.11.2017

signature



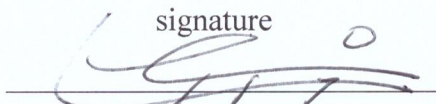
Advisor: Young-Nam Kwon

signature



Chang Ha Lee : Thesis Committee Member #1

signature



Jae Weon Cho : Thesis Committee Member #2

Abstract

As a water treatment technology, the membrane distillation (MD) method which can operate at lower temperature than reverse osmosis (RO) and can recover concentrated water generated from RO with high recovery rate has been studied. Membrane distillation is a technology that allows the vaporized water pass through membrane pores and collect pure water vapor so that many types of research has been studied.

In this study, a hollow fiber was made using Poly(vinylidene fluoride-co-chlorotrifluoroethylene) (PVDF-CTFE), not usually used material, and compared with Poly(vinylidene fluoride) (PVDF). There is four type of membrane distillation methods. Among them, the vacuum membrane distillation method which has the highest flux method was studied in this research. In the case of PVDF-CTFE, it was confirmed that it has a higher flux because it has a macrovoids at lumen side than PVDF. However, since the mechanical strength is weak, there is breaking problem when operating long term experiment or high-pressure experiment.

To solve the breaking problem, the mechanical strength was increased by using thermally induced phase separation (TIPS) method, which is a high-concentration spinning method, or by spinning hollow fibers into a dual-layer structure in which PVDF is spun out as a support layer. In the case of TIPS, the mechanical strength was increased, but the flux was found to be low. As can be seen from the cross-sectional images of the hollow fiber, in the case of the dual-layer membrane, the sponge-like structure at the middle was eliminated, and the flux was improved.

Furthermore, to prevent the wetting phenomenon of membranes, physical and chemical modification experiments were carried out to increase hydrophobicity. First, a hydrophobic hollow fiber was prepared by physically blending with Polytetrafluoroethylene (PTFE), which is a highly hydrophobic material, in a dope solution, and physical properties were confirmed. PTFE was added as an additive to evaluate the structural change and performance. As a method of increasing the hydrophobicity using the chemical grafting method, attaching a hydrophobic chemical to the surface of the polymer using the atom transfer radical polymerization (ATRP) method was used. The chemical method was used to evaluate the performance by confirming the difference according to the length of the material with different reaction time.

Both methods were confirmed physical property changes via FTIR and confirmed the increase in hydrophobicity through contact angle and liquid entry pressure (LEP). Through the physical blending method, it was confirmed that the contact angle was improved by the addition of the hydrophobic

additive. Also, the cross-section of the hollow fiber was confirmed by SEM, confirming that the pores of the membrane became larger at lumen side. However, if more than 15 wt% of PTFE is contained, the sponge-like structure is formed again in the middle of the hollow fiber, and it becomes thicker depending on the PTFE content. As a result of this structural change, the flux was affected, and the flux was improved up to 10 wt%.

Through ATRP, which is a chemical modification method, it was confirmed that a new peak of FTIR and XPS appeared on the polymer by grafting hydrophobic material. After grafting, membrane structural change was checked by SEM that there was no change of pore, the hydrophobicity was confirmed by the contact angle that there was increasing contact angle value, the flux was confirmed through the membrane distillation method that was no improvement. Increasing of hydrophobicity contributes to preventing the wetting problem that checked through LEP. With increasing reaction time, LEP value increased until 5 bars.

Finally, the performance evaluation was carried out through the hollow fiber obtained by combining the two methods. The 10 wt% PTFE blended hollow fiber with the highest flux was prepared, and ATRP was carried out for 25 hours. In the case of the hollow fiber obtained, the flux is maintained as in the case of blending 10 wt% of PTFE, and the LEP is further increased which can be confirmed that the wetting phenomenon can be prevented.

Contents

Abstract.....	i
Contents	iii
List of Figures.....	v
List of Tables.....	viii
Chapter 1. Introduction.....	1
Chapter 2. Background	4
I. Desalination methods	4
1.1 Several types of distillation methods	4
1.2 Reverse osmosis (RO)	5
1.3 Membrane distillation (MD)	7
II. Development of hollow fibers for MD	9
III. Fabrication of hollow fibers for MD.....	11
1.1 NIPs (Non-solvent induced phase separation).....	11
1.2 TIPs (Thermally induced phase separation)	12
Chapter 3. Materials and methods	14
I. Materials.....	14
II. Preparing for the experiment	15
2.1 ATRP for Synthesis of Hydrophobic Substance	15
2.2 Hollow fiber spinning	15
2.3 VMD.....	16
III. Characteristic	17
3.1 Scanning electron microscopy (SEM)	17
3.2 Attenuated total reflectance-Fourier transform infrared spectroscopy (ATR-FTIR) ...	18
3.3 Water contact angle	18
3.4 Measurement of Mechanical property	18
3.5 Viscosity measurement	18
3.6 Liquid Entrance Pressure (LEP).....	18

3.7 X-ray photoelectron spectra (XPS)	19
3.8 VMD Performance Evaluation	19
3.9 Direct contact membrane distillation (DCMD) for evaluate wetting degree.....	19
Chapter 4. Results	21
I. Polymer selection	21
1.1 Background of PVDF-CTFE selection	21
1.2 Single-layer hollow fiber spinning	24
1.3 Measurement of tensile strength and VMD flux	28
II. Spinning for Strength Improvement	31
2.1 Spinning dual-layer hollow fibers.....	32
2.2 Spinning through the TIPs method	37
III. Spinning dual-layer hollow fibers for enhancement of hydrophobicity	41
3.1 Improving hydrophobicity through blending PTFE as an additive	41
3.2 Improvement of flux of dual-layer hollow fiber membrane through ATRP	48
VI. Fabricate dual-layer hollow fibers with combined chemical and physical methods	55
4.1 VMD performance test through LEP and flux measurement.....	55
4.2 Wetting experiment through DCMD	60
Chapter 5. Conclusions.....	62
Reference	64

List of Figures

Fig. 1 Polymer for hollow fiber and ATRP reagent. (a) Polymer PVDF as a hollow fiber membrane, (b) Polymer PVDF-CTFE as a hollow fiber membrane, (c) Reagent pentafluorostyrene for chemical grafting.....14

Fig. 2 Schematic diagram for ATRP method.....15

Fig. 3 Equipment for spinning. (a) Bore solution, (b) Pump for bore solution, (c) Inner dope solution tank, (d) Outer dope solution tank, (e) Triple-layer spinneret, (f) Coagulation bath, (g) Washing bath, (h) Wind up.16

Fig. 4 Schematic diagram for VMD.....17

Fig. 5 Comparison of contact angle value with various polymers.....22

Fig. 6 ATRP changes checked by FTIR for several polymers. (a) PVC with styrene, (b) PVDF with styrene, (c) PVDF-CTEF with styrene.23

Fig. 7 Comparison of dope polymer solution’s viscosity at each concentration.25

Fig. 8 Cross-sectional images for single-layer hollow fibers. (a) PVDF 17 wt% cross-section, (b) PVDF shell side, (c) PVDF lumen side, (d) PVDF-CTFE 28 wt% cross-section, (e) PVDF-CTFE shell side, (f) PVDF-CTFE lumen side.....27

Fig. 9 Comparison of VMD flux for each single-layer hollow fiber.29

Fig. 10 Comparison of each hollow fiber’s LEP.....30

Fig. 11 Cross-sectional images for dual-layer hollow fiber. (a) Dual-layer cross-section, (b) Lumen side of hollow fiber which is PVDF-CTFE, (c) Shell side of hollow fiber which is PVDF, (d) Lumen side of hollow fiber which is PVDF-CTFE, (e) Shell side of hollow fiber which is PVDF.....33

Fig. 12 Comparison of VMD flux for single & dual-layer hollow fibers. .35

Fig. 13 Comparison of LEP which affect to hydrophobicity.....36

Fig. 14 Cross-sectional images for TIPs. (a) 28 wt% of PVDF-CTFE, (b) 35 wt% of PVDF-CTFE, (c) 40 wt% of PVDF-CTFE.....38

Fig. 15 VMD flux comparison for TIPs hollow fibers which spun at different polymer concentration.40

Fig. 16 FTIR peak comparison with different concentration of PTFE. ...42

Fig. 17 Comparison of contact angle with different PTFE concentration.43

Fig. 18 Viscosity by PTFE concentration.....44

Fig. 19 Comparison hollow fiber’s cross-sectional images with different PTFE concentration. (a) Pure dual-layer hollow fiber, (b) Lumen side image for 5 wt% of in inner dope solution, (c) Lumen side image for 10 wt% PTFE in dope solution, (d) Lumen side image for 15 wt% PTFE in dope solution, (e) Lumen side image for 20 wt% PTFE in dope solution.45

Fig. 20 Comparison of VMD flux change by different PTFE concentration.46

Fig. 21 Change of LEP due to different PTFE concentration.....47

Fig. 22 Comparison of FTIR peaks after ATRP reaction. (a) Change in inner peak of hollow fiber according to ATRP time, (b) Change in outer peak of hollow fiber according to ATRP time.....49

Fig. 23 XPS results following by different ATRP reaction times. (a) XPS C, (b) XPS Cl.....50

Fig. 24 Comparison of contact angle change with different ATRP synthesis time.51

Fig. 25 Cross-sectional images after ATRP. (a) 15 hours ATRP reaction, (b) 20 hours ATRP reaction, (c) 25 hours ATRP reaction.52

Fig. 26 Comparison of flux according to different reaction time.52

Fig. 27 LEP change with synthesis time.54

Fig. 28 FTIR peak result after blending and grafting method. (a) PVDF-CTFE-g-PFS synthesis 25 hours which add PTFE 10 wt% before spinning, (b) Outside surface of modified hollow fiber membrane...56

Fig. 29 Cross-sectional images of modified hollow fiber with combined physical and chemical modification method. (a) Dual-layer hollow fiber with PTFE 10 wt%, (b) Dual-layer hollow fiber with PTFE 10 wt% after 25 hours ATRP.....57

Fig. 30 Comparison of VMD flux with single, dual-layer, modified dual-layer hollow fiber membranes.....58

Fig. 31 LEP comparison of LEP with single, dual-layer, modified dual-layer hollow fiber membranes.....59

Fig. 32 Comparison of wetting time through DCMD.61

List of Tables

Table. 1 Conditions for VMD.	17
Table. 2 Comparison of viscosity at different polymer concentration.	24
Table. 3 Spinning conditions for dual-layer hollow fiber.	26
Table. 4 Comparison of single-layer hollow fiber's mechanical strength.	28
Table. 5 Conditions for spinning dual-layer hollow fiber.	32
Table. 6 Comparison of mechanical strength for single and dual-layer hollow fibers.	34
Table. 7 Conditions for spinning with TIPs method.	37
Table. 8 Comparison of mechanical strength for single-layer hollow fibers spun with TIPs method.	39

Chapter 1. Introduction

Due to the increase in population, the usage of clean water is continuously increasing. From 1900 to 1995, the population doubled, but the demand for water increased by six (Kuylenstierna et al., 1998). In many places, the increase in the activities of industry and agriculture also contributes to the increase of water consumption. As the use of water increases, many countries suffer from water shortage. However, in the case of rivers and groundwater, which are available resources for obtaining clean water available, the consumption of water will continue to increase in this situation. As a result, the researches on the technology for purifying the used water to obtain clean water have been rapidly proceeding.

There are several types of desalination methods, distillation and reverse osmosis (RO) have been used. As a technology to generate clean water, technology using sea water which occupies 97% of the earth has been popular. In the case of seawater, which occupies a large part of the Earth, it can not be used directly or commercially. Therefore, many seawater desalination techniques have been researched to remove the salts. Distillation is a typical method used for seawater desalination. In the Middle East, evaporation is used as an important way to obtain clean water (Alawadhi, 2002). It is a technique to obtain pure water by separating the salt water containing salt from the salt by using evaporation and has the advantage of not requiring high pressure. The speed at which water is produced is proportional to the area, but it needs high thermal energy. Also it has a disadvantage that production speed is slower than other methods (Tiwari et al., 2003). There is another technology; RO is one of the most widely used technologies of seawater desalination. The largest seawater Reverse Osmosis (SWRO) plant currently on the Ashkelon Israel has been the most studied technology in recent decades. It produces 110 million/m³ of water per year, which is enough to supply to 100,000 people (Hoekstra and Chapagain, 2008). It is a disadvantage in that higher pressure is needed than the osmotic pressure to make pure water from semipermeable membranes. Also, it is an important factor to solve the cost problem of seawater desalination technology using RO in poor countries because it requires such high pressure.

Previously, seawater desalination technology has been studied to produce water through distillation and RO. However, the evaporation method which obtains the clean water by the heat evaporation does not solve the problem of the low production amount, and the RO using the osmotic pressure can not solve the problem requiring the high pressure. As a method to solve these problems, a membrane distillation (MD) method has been got attention. The MD is a method of using water to induce the evaporation of water according to the temperature difference of the solutions and passing the evaporated vapor pass through the membrane to produce pure water. This method can solve the problem of high temperature or high pressure, which is a problem of the previous distillation method and RO, and can be operated at a low temperature and does not require high pressure. Also since only water vapor passes through the pores, it is theoretically having a salt removal rate of 100%. MD was first introduced by

Bodell in 1963 (Bodell, 1963). Since then, interest in MD has been increasing. As previously introduced, MD is a method of collecting vaporized vapor which induced by thermal differences. The membrane acts as a barrier between the two solutions. At this time, the pores existing in the membrane give a path through which vaporized vapor can pass. However, if the water vapor coagulates in the pore and wet the membrane, the water vapor will no longer pass through the pores and the efficiency will be reduced. Therefore, the hydrophobicity of the membrane is a very important factor for membrane distillation (Gryta, 2007).

To prevent such wetting phenomena, hydrophobic materials have frequently been used in MD. Usually, PTFE, PP, and PVDF are used for membrane (Khayet and Matsuura, 2001). However, there is a limitation in using only hydrophobic polymers to overcome wetting phenomenon. Therefore, there have been many studies to further increase the hydrophobicity. Modification methods of membranes include physical blending methods and chemical grafting methods. A hydrophobic membrane can be made using physical blending methods as an easy modifying method. A study on the improvement of hydrophobicity by selecting PTFE as an additive was studied by May May Teoh (Teoh and Chung, 2009). The effects of PTFE with high hydrophobicity and excellent chemical resistance on the membrane distillation method were investigated by spinning single PVDF hollow fiber membranes. In their study, the contact angle increased to 103° with the addition of 50 wt% of PTFE and the maximum flux of 40.4 LMH ($L/m^3 \cdot \text{hour}$) was obtained in DCMD (Direct Contact Membrane distillation). In subsequent studies, the efficiency of DCMD was increased by increasing hydrophobicity by blending PTFE in the dope solution of the outer layer when spinning the dual-layer hollow fiber (Teoh et al., 2011). The same PVDF solution was spun using a triple-layer spinneret. When 30 wt% of PTFE was added to the outer dope solution, it was confirmed that the flux enhancement was 24% higher than when PTFE was added to a single-layer hollow fiber membrane. In their study, there was structure change with increase PTFE concentration, but also decrease flux because of the sponge-like structure. Additive with high hydrophobicity changed structure, so that affect to flux. To solve decreasing flux because of structure change, experiments have also been carried out with chemical grafting method. Through chemical grafting method, there are no changes and can increase hydrophobicity. Studies have been done to increase hydrophobicity by synthesizing styrene to PET through ATRP by Bech (Bech et al., 2009). It was confirmed by XPS, H NMR, ATR-FTIR, and contact angle value that the longer branches were formed as the synthesis time increases. After 6 hours of synthesis, modified membrane (87.9°) has more high contact angle value than Pure PET membrane (77.8°). Also Manal conducted an experiment to improve the efficiency of vacuum membrane distillation (VMD) by synthesizing ethyl acrylate (EA) on PVC (Tooma et al., 2015). In their work, they have experimented to increase the efficiency of VMD by increasing the hydrophobicity of the membrane through synthesizing EA on PVC. The hydrophobicity was improved by having a contact angle of 90° which is 10° higher than that of pure

PVC. In the case of flux, it was confirmed that the pre-modification PVC membrane had a flux of 37.5 LMH in the case of the modified PVC membrane, while it had a value of 2.52 LMH in the pre-modification PVC membrane. Previously, the experiments of increasing the hydrophobicity through the chemical grafting was successful. However, only the contact angle test was carried out by confirmation of the result of increase in hydrophobicity, and the experiment related to the wetting phenomenon of MD did not proceed.

Previously, experiments were conducted to increase hydrophobicity through physical blending and chemical grafting. However, it did not solve the problem of flux reduction because of structural change due to the additive. Also it has not been solved that the experiment about the prevention of the wetting phenomenon of the MD due to the increase in hydrophobicity has not been carried out. To overcome this kind of problem, experiments were conducted using PVDF-CTFE, which is a polymer that has higher hydrophobicity than PVDF itself and can easily be chemically grafted due to the functional groups present in the polymer. PVDF-CTFE is a polymer that is not widely used as a material for MD but has a higher hydrophobicity than PVDF and has a Cl functional group so that it can be easily combined with a hydrophobic material through a chemical bonding method.

The purpose of this study is to fabricate the hydrophobic hollow fiber membrane for MD and evaluate the performance of membranes on VMD. The PVDF-CTFE was spun in the form of a hollow fiber. The hollow fiber membrane was evaluated by the VMD method. To further increase the hydrophobicity of the membrane, experiments on the modification by physical and chemical methods were carried out. For physical blending method, PTFE was used as a hydrophobic additive. Structural and performance changes were observed according to the amount of added PTFE. Structural changes were observed by SEM and hydrophobicity was confirmed by contact angle and LEP. Pentafluorostyrene, which has a benzene ring and hydrophobic functional groups, is used as a reagent for the chemical grafting method. As a grafting method, C functional group in PVDF-CTFE was dropped through ATRP method and replaced with pentafluorostyrene. Also the difference of the length of branches along the synthesis time was confirmed by FTIR, XPS, contact angle, and LEP.

Chapter 2. Background

I. Desalination methods

1.1 Several types of distillation methods

As mentioned above, the usage of clean water is continuously increasing due to the increase in population (1997). For the production of clean water, sea water technology, which accounts for 97% of the earth, has been popular. Various seawater desalination techniques have been studied as techniques for removing salts present in seawater. One example is the evaporation method, which is a representative technique used for seawater desalination. The evaporation method is a seawater desalination technology that has been known since the 4th century BC, and the modern desalination system is the first in the late 19th century (Tiwari et al., 2003). The land facility started to supply water from the desert during World War II. Since the 1950s, the desalination system has become bigger and bigger in the Middle East. When the sea water is evaporated, the solvent water evaporates, and the salt, the solute, separates the fresh water from the seawater by using the remaining property. Multi-stage flash distillation (MSF), multi-effect distillation (MED), and mechanical vapor compression distillation (MVC) are classified according to evaporation method and steam recycling method.

1.1.1 Multi Stage Flash Distillation

The multi-stage flash method (MSF) is currently the most widely used desalination technology for large capacity desalination plants, accounting for about 60% of the global desalination capacity (Fritzmann et al., 2007). When the liquid at a certain temperature is suddenly decompressed to a saturated vapor pressure corresponding to the temperature, the liquid consumes the retained heat as the latent heat of evaporation, thereby causing self-evaporation or flash evaporation. In the multi-stage flash system, the seawater heated in a relatively high-pressure heat exchanger is evaporated through the orifice into the low-pressure compartment, and the heat energy of the whole is evaporated. In this case, since there is no heat supply from the outside in each compartment. The amount of evaporation in each compartment is within a few percent.

1.1.2 Multi effect distillation

Multi-Effect Distillation (MED) is a series of simple distillers (Khawaji et al., 2008). The vapor generated in the first evaporator boiler acts as a heating source for the next utility evaporator and is cooled and condensed to become fresh water. The steam generated in the second evaporator acts as a heating source in the evaporator of the next utility, thereby evaporating seawater in the evaporator. In other words, the steam received from the shear becomes the heat source of the next stage, and the steam is cooled and condensed to become fresh water, and the steam evaporated again is collected at the next stage as fresh water. It has a much lower energy consumption than the MSF method and shows a large output (M.A. Darwish, 1995). Therefore, it shows higher efficiency than MSF regarding thermodynamics and heat exchange.

1.1.3 Mechanical vapor compression distillation

Mechanical Vapor Compression Distillation (MVC) is a method in which steam generated in an evaporation tank is introduced into a compressor, the temperature is raised by adiabatic compression, and the steam is supplied to the steam for heating the liquid in the same tank to obtain fresh water (Shaffer et al., 2013). When the steam generated in the evaporation tank is compressed by a compressor, the temperature and pressure rise, which is used as a heat source of the evaporator. The sensible heat of the brine and the produced fresh water discharged from the seawater through the heat exchanger is recovered. The condensed vapor evaporates by the heat it emits as it condenses, and the vapor is again condensed in the evaporator at a high temperature (105 °C) with the compressor and then passes through the heat recovery system and transfers the sensible heat to the seawater entering the evaporator. It is known that steam compressors can produce more than 200 kg of fresh water per kg of fuel when the compressor is driven by a small engine and the waste heat is utilized. This MVC method has advantages mainly in small capacity desalination devices.

1.2 Reverse osmosis (RO)

However, in the case of the evaporation method, a high temperature is required, and the efficiency of the production is not so high as compared with other methods. A reverse osmosis method has been studied as a method to solve these drawbacks. RO is one of the most used technologies of seawater desalination. The technology has been the most studied in recent decades. Research on osmotic pressure, RO, has been conducted since 1985 (Cadotte, 1985). Cadotte conducted research on the materials that make up the membrane and focused on the composite RO membrane. Also a study using chemical properties of cellulose acetate (CA) was conducted in 1950. The CA membrane with hand-made symmetric structure has the advantage of maintaining the salt removal rate at 98%, but it can not solve

the low flux (Reid and Breton, 1959). Therefore, as a material to solve this problem, the membrane using cellulose triacetate (CTA) has been selected as a material to withstand a wide range of temperature and pH. Research has been carried out on the advantage of resistance to high chemical and biological attack, but it has been confirmed that severe flux reduction is caused by compaction even at a high pressure of 30 bars (Porter, 1989). Due to these problems, by 1969, CA was the most suitable material for the RO. However, due to the hydrolysis of the acetate group under acidic and alkaline conditions, there is a problem of being susceptible to microbial contamination, and the durability and application range are limited (Edgar et al., 2001). This has led to research into alternative polymers with stronger chemical durability.

For the first time, a study on hollow fiber membrane using aromatic polyamide (PA) as a non-cellulosic asymmetric membrane was developed by Richter and Hoehn (Hoehn and Richter, 1980). CA, but the durability and stability were much more remarkable, and due to the characteristics of the hollow fiber, it was commercially successful due to efficient packing. However, PA has also been found to be vulnerable to chlorine and ozone. To solve this problem, development of an asymmetric membrane using polypiperazine-amides has been developed (Credali et al., 1978). It has a selective permeability comparable to CA and is resistant to chlorine attack. However, it has a relatively low salt removal rate (< 95%). Therefore, to solve the problem of salt removal rate, sulfonated polysulfone with sulphonic and phenyl groups was used as a suitable polymer for enhancing permeability, mechanical strength, and chemical resistance. However, there is a problem that the salt removal rate is lowered to be commercialized (Brousse et al., 1976).

Only a few soluble polymers were able to make the film through one step of the asymmetric structure. However, the membrane through this method did not show proper performance regarding permeability and salt removal rate. To solve this problem, the membrane was made through two steps. A study has been made on a membrane having a structure which is optimized as a layer having a large pore as a support layer and a barrier layer for removing salt, respectively. The development of a thin film composite membrane (TFC), which consists of a thin layer as the barrier layer and serves as a supplementary layer with large pores, was first developed by Francis (Francis et al., 1966). Since then, many studies have shown that polysulfone as a supplementary layer material has been selected for its resistance to compaction and its resistant flux (L.T. Rozelle, 1968). The material is also more popular because of its durability in acidic conditions. The use of polysulfone as a support layer opens the way for interfacial polymerization. This material is now available because of its resistance to alkali. The first attempt was made to synthesize aliphatic and aromatic diamines. However, this membrane did not show the salt removal rate that attracted attention (Petersen, 1993). Studies have been conducted to solve the problem of salt removal rate, and Cadotte has found that excellent selective permeability can be obtained using monomeric aromatic amines and aromatic acyl halides (Cadotte, 1981). Unlike other

interfacial polymerization methods, it avoids curing and does not require acid acceptor or surfactant. Acyl halide is rapidly supplied and polymerization and crosslinking occur. This innovative cross-linked aromatic polyamide TFC RO membrane has been extensively studied and has been widely used until the 1980s.

1.3 Membrane distillation (MD)

Many water treatment technologies have been studied. However, it is possible to operate at low pressure, but the problems of evaporation methods with low production volume and RO methods requiring high pressure have not been solved. As a method for solving this problem, there is a membrane distillation method using a thermally driven method. This method is a method that can obtain only pure steam by evaporating water using heat. At this time, the membrane serving as the intermediate diaphragm is made of a material having a hydrophobic characteristic. Membrane distillation can be operated at a low temperature and by using the driving force due to the temperature difference between the two solutions, the vapor can be obtained without boiling the treatment solution to the boiling point (Alkudhiri et al., 2012). MD, first introduced in 1963, was studied by Bodell (Bodell, 1963). In his work, we proceeded with the use of a silicon membrane, but could not confirm the geometry or state of the pore. The air was sent to the lumen and only the water vapor was condensed outside the membrane through the membrane, which was shown to increase the efficiency by hanging the vacuum outward, but the membrane tube was broken and failed to run. In 1967, the study of MD was carried out by Weyl for the purpose of increasing the efficiency of seawater desalination (Weyl, 1967). A flux of 1 LMH was obtained using a PTFE membrane with a thickness of 3.2 mm and a pore size of 9 μm . However, it was only slightly interested because it was lower than RO with flux of 5 to 75 LMH.

Findley first published about the basic theory of distillation and DCMD for the first time in the 1960s (Findley, 1967). Since then, researches on MD have been continued, and further studies have been conducted to improve the module design and understand the temperature and concentration polarization phenomena (Gore, 1982). Also, for commercial use, experiments were carried out on MD using Membrane manufactured by The Swedish development Co (Carlsson, 1983). In this study, a spiral wound module was fabricated to solve the heat transfer problem. Commercial studies were conducted by Enka in the 1980s. Since then, MD has received much attention in academic. The published research on MD has shown that it increased about twice in 1997 compared to 1990 (Sirkar, 1992). These membrane distillation methods are divided into 4 types depending on the type.

1.3.1 DCMD (Direct Contact Membrane Distillation)

DCMD is a widely used method because it is a convenient and easy method compared to other methods of MD. The solution that is cooler than the feed solution maintains the temperature and flows to the opposite side of the membrane boundary. At this time, due to the temperature difference between the two solutions, water vapor is generated in the hot feed. The generated water vapor passes through the pores of the membrane to the opposite side. The water vapor that passes through the pore is a way of condensing again as it meets the cold permeate on the opposite side. This is because the evaporation of water vapor in the module takes place in the module, which is the easiest way to do so, unlike the SGMD or VMD, which requires no additional external condensation system. However, there is a problem of heat loss due to heat exchange between feed and cold permeate. DCMD has been used in many fields such as enrichment of fruit juice, blood, wastewater treatment (Schofield et al., 1990). DCMD was first used in 1964 for seawater desalination (Weyl, 1967). However, a problem was found to have a lower flux than the RO method. To solve the problem of low flux, the ongoing research was continued, and it was possible to improve the flux to 75 LMH which is comparable to that of RO, and the salt removal rate was close to 100% (Schneider et al., 1988).

1.3.2 AGMD (Air Gap Membrane Distillation)

Another type of MD is AGMD. To reduce the heat loss, a method of increasing the heat efficiency, which is lower than that of DCMD, is a method in which an air layer is formed between the membrane and a cold surface for condensation while flowing through the membrane. The evaporated water vapor is condensed on a cold surface and collected through pores. Moreover, an air layer is provided there between. When the evaporated water molecules pass through the pores, the cold permeate touches the flowing surface and condenses and falls. The cold surface is located away from the membrane, and the heat loss is relatively small compared to DCMD. However, it has a disadvantage that it has a relatively low flux due to the generation of water vapor due to pure heat evaporation. This method can confirm that feed temperature, flow rate, concentration, and deaeration affect DCMD in a similar way (Jönsson et al., 1985).

1.3.3 SGMD (Sweep Gas Membrane distillation)

MD also has the form of the SGMD method. SGMD was developed as a solution for DCMD and AGMD. SGMD is the result of a combination of low heat loss of AGMD and reduced transport resistance of DCMD. In the case of AGMD, a gas barrier exists between the membrane and the cold surface, which results in reduced heat loss. However, in the case of SGMD, the flow of air rather than the stopping air layer improves the mass transfer constant and increases the flux. The vapor that flows

through the evaporation-accelerating gas travels continuously and the gas must flow continuously to re-condense the circulating gas. At this time, there is a considerable expense to flow the gas for the SGMD. Therefore, DCMD has not received much attention than DCMD. In the case of SGMD, it was confirmed that it was not affected much by the temperature of the gas flowing and was influenced by the velocity (Basini et al., 1987). It was confirmed that the flux tends to increase as the gas velocity increases. However, the flux tends to decrease as the gas velocity increases above the optimum point.

1.3.4 VMD (Vacuum membrane distillation)

Finally, there is VMD as a vacuum MD. This method is the least studied of the MD method. It keeps the temperature of the feed and the pressure on the permeate side is vacuumed to lower the boiling point of the solution of the feed, thereby inducing evaporation of the feed solution to increase the flux. The evaporated water vapor passes through the pores of the membrane to permeate and condenses on the cold condenser side to purify. This method is advantageous in that it has less heat loss because the cold condenser is separated from other methods. Also, the mass transfer resistance is reduced due to the vacuum, so that the flux is high. However, it is a complicated technology and has a disadvantage of high cost for vacuuming. The effects of feed temperature, velocity, and concentration on flux were similar to DCMD and flux was studied by Sarti (Sarti et al., 1993). This VMD method is widely used as a process for removing volatile substances from a diluted solution. The study was also conducted by Bandini as a process for separating ethanol using thermally driven through the vacuum (Jonquière et al., 2013). In his study, the concentration of ethanol was found to be about 10 times higher than that of AGMD.

Depending on the type of condensation, the MD can be divided into four types. The most studied method is DCMD, and the most fluxed method is VMD. All of the four methods described above are methods to purify by inducing evaporation using thermal difference, and steam generation is an important factor. However, as steam passes through the membrane, pores become wet. This wetting is one of the important problems to be solved in the MD. To solve the wetting phenomenon, the hydrophobicity of the film plays an important role. To this end, many types of research have been made on the material for making the film and the modification of the material.

II. Development of hollow fibers for MD

PP, PVDF, PTFE, etc., which have hydrophobic characteristics, are used as the materials used in the membrane distillation method described above. The reason for using the material having the

hydrophobic characteristic is to reduce the wetting phenomenon. The pores present in the membrane are the lengths through which the evaporated water vapor can pass, but if the water vapor moving through the pores coagulates in the pores and makes the membrane wet, the water vapor will no longer pass through the pores and the efficiency will drop. Therefore, the hydrophobicity of the membrane is a very important factor for membrane distillation. Membranes for membrane distillation can be made in the capillary or flat-sheet form (Ding et al., 2003). Compared with other membrane separation processes, the study on high flux and low resistance was carried out (Lawson and Lloyd, 1997). It has the largest area per unit area than other types of membranes and has the advantage that separation is not caused when the membrane is washed because no support layer is needed to make it. It also has the advantage of the operational flexibility that can be used in many areas such as RO, UF, MF, hemodialysis, and gas separation. However, it takes a complicated preparation to form the film. The size of the aperture of the spinneret was used, the rate at which the dope solution emerges, the length of the air gap, and the take-up speed of the spun hollow fiber.

Studies on the effects of dope type, bore solution type, temperature, dope and bore on the fabrication of hollow fiber have been studied (Cabasso et al., 1976). Some studies that affect the formation of hollow fibers have been conducted by Tai-Shung Chung on the effects of shear rate on morphology, permeability, and segregation performance (Chung et al., 2001). In the case of the dope solution with a high shear rate, it was confirmed that a thick, dense membrane was produced. It was also confirmed that the flux decreased and the heat exchange constant also decreased. However, it was confirmed that the mechanical strength was increased. A study of the influence of the other factor, air gap, has also been carried out (Mok et al., 1995). As the spinning method using the dry-jet wet method, the dope solution starts to come out from the spinneret, but when it starts to solidify, the inside of the spinneret starts to solidify. However, in the case of outside, it takes time until reaching the external coagulation bath. Research has been conducted. It is reported that the permeability decreases when the air gap is increased (Aptel et al., 1985). Recent studies show that as the air gap increases, the hollow fibers become thinner and dense sponge-like structures. These results show that the permeation flux decreases and the salt removal rate increases.

A study on the change of hollow fiber structure by adding physical additives was also carried out. Membrane preparation through a blending of additives has the advantage of being simple and ready for mild conditions. A study on the performance change of PVDF hollow fiber membranes using LiCl and PEG as additives was conducted by D. Hou (Hou et al., 2009). As LiCl and PEG were added, the shape of the finger-like structure became longer on the cross-section of the hollow fiber. Also, it was confirmed that the performance of MD is improved by forming a thin skin and porous structure. Studies on TiO₂ as another additive were also carried out (Yuliwati et al., 2011). In the case of TiO₂, the hydrophilicity of the membrane was increased, the pore size was decreased, and porosity was observed.

It was also confirmed that the flux increased with increasing pH. Studies on the addition of SiO₂ as another additive were also carried out. Higher flux and stronger mechanical strength were obtained with addition (Han et al., 2010). Studies on the addition of Al₂O₃ have also been carried out, and further studies have been carried out by Liu when added with TiO₂ (Chiang et al., 2004). Studies on the addition of PVP as a hydrophilic additive also proceeded (Fontananova et al., 2006). As the concentration of PVP in the dope solution increased, the macrovoids gradually increased as the cross-section was observed. This study showed that PVP with high hydrophilicity was rapidly exchanged with external coagulation bath to produce large macrovoids.

Increasing hydrophobicity through previous physical additions has many variables and limits that are affected by the properties of the additives. Due to these limitations, research has been carried out to increase the hydrophobicity of the polymer through chemical bonding of highly hydrophobic materials. On the PE membrane, MMA was synthesized through atom transfer radical polymerization (ATRP) method (Shi et al., 2013). It was confirmed that the degree of bonding increases with the synthesis time and that the length of the PMMA becomes longer. As a result, the hydrophilicity becomes larger as the contact angle becomes smaller. Research has been carried out to increase the hydrophilicity, but studies have also been conducted on the chemical bonding to increase the hydrophobicity to prevent the wetting phenomenon of the membrane distillation method. Mingfu conducted a successful combination of styrene or tert-butyl acrylate by dropping the Cl functional group of PVDF-CTFE through the widely used ATRP method (Zhang and Russell, 2006). The benzene rings of styrene are hydrophobic due to their structural properties. The research through ATRP was carried out as a method to make such a hydrophobic branch long.

Much research has been done on the effect of physical blending or chemical grafting on the performance of membranes by changing the structure or polymer properties. In addition to changing the properties of materials to make these films, much research has been done on the preparation of solutions for preparing membranes.

III. Fabrication of hollow fibers for MD

1.1 NIPs (Non-solvent induced phase separation)

In addition to studying the performance change of the membrane by using the additives of the above-mentioned membrane or chemical bonding, researches have been carried out in accordance with the method for making the membrane. In the case of NIPs, it is a method of producing an asymmetric membrane by exchanging between solvent and non-solvent (Yun et al., 2012). The most common method for fabricating porous membranes is known as the phase transformation method first introduced

by Kesting. The method of inducing the phase transition of the polymer solution is largely solvent-non-solvent exchange, heat induction, and steam induction method. Among them, the precipitation of the polymer by exchange of the solvent and the non-solvent is used for the commercialization of the microfiltration membrane or the ultrafiltration membrane, and it is most widely used for manufacturing.

In the solvent, non-solvent exchange method, a homogeneous solution is prepared by dissolving a polymer material in an appropriate solvent at room temperature, and a hollow fiber is drawn from that spinneret, and then immersed in a coagulation tank. Then, the exchange of solvent and non-solvent are carried out in the coagulation tank, and the composition of the polymer solution is changed. As a result, the polymer is precipitated by liquid-liquid phase separation beyond the binodal or spinodal curve which shows the solubility limit, and the part where the non-solvent was occupied is formed by the pore (Bonyadi and Chung, 2009). It is known that liquid - liquid phase separation proceeds in two forms. That is, at the moment when the liquid-liquid phase separation occurs very rapidly, the composition of the solution passes through the binodal curve under the phase separation, and a structure having finger-like structure is formed. This condition corresponds to the case where the interaction between the non-solvent and the solvent is very large, and the prepared membrane is mainly used as a reverse osmosis membrane or an ultrafiltration membrane. On the other hand, another microfiltration membrane is produced by delayed phase separation, in which the exchange of non-solvent and solvent is very slow, and a sponge-like symmetric membrane without finger-like structure is mainly formed. In some cases, experiencing steam-induced phase separation before coagulation of the non-coagulant precipitate can produce a finger-like structure membrane. This is a method that can spin and maintain the temperature at room temperature and can radiate easily to use a low concentration of polymer. However, there is a disadvantage in that the mechanical strength is low due to the low concentration of the polymer and the large pores, which can not withstand a large pressure.

1.2 TIPs (Thermally induced phase separation)

To solve the problems of the previous NIPs, it is necessary to develop a membrane having excellent mechanical strength. One method to solve this problem is the thermal induction phase transition method, which mainly uses a crystalline polymer having excellent chemical resistance and mechanical strength. In the TIPS process, a homogeneous single-phase melt is prepared at a temperature higher than the melting point of the polymer; the polymer is formed into a hollow fiber, and the phase is cooled by removing the applied heat to induce phase separation (Cabasso et al., 1976). In the heat - induced phase separation method, cooling rate, and solidification conditions are known to be very important factors for determining the film structure. As the interaction increases, the crystal size decreases and the porosity of the film increases. On the other hand, when the quenching temperature is low, or the cooling

rate is high, a small quartz is formed. When the quenching temperature is high, or the cooling rate is slow, a large quartz is formed. This is because crystallization slowly proceeds when the quenching temperature is high or the cooling rate is low, which is a favorable condition for the crystal to grow sufficiently.

The membranes obtained through the TIPS process have advantages over the membranes prepared by the NIPs method regarding mechanical strength and chemical resistance. However, the NIPs method is capable of micro pore control while the TIPS method still has a disadvantage in that it is difficult to fabricate an ultrafiltration membrane having a finger-like structure, and since the spinning hollow fiber must be maintained at a high temperature during fabrication (Cha and Yang, 2007).

Chapter 3. Materials and methods

I. Materials

In this study, polymers with high hydrophobicity were selected for spinning. PVDF-CTFE (polyvinylidene fluoride-co-chlorotrifluoroethylene) was used to make hollow fibers. PVDF-CTFE has an excellent electromechanical response, high flexibility, high elongation, and cold impact resistance properties. In this study, we investigated the effects of spinning high-hydrophobicity hollow fibers through PVDF-CTFE on the membrane distillation process by using modified PVDF-CTFE. PVDF is also a polymer with high chemical resistance and high mechanical strength and can be expected to have high hydrophobicity due to its F functional group.

As shown in Fig. 1 (a), (b), PVDF-CTFE (PVDF SOLEF 31508/1001) and PVDF (PVDF SOLEF 1015/1001), which are polymers used as materials for making hollow fibers, were used. As a solvent for dissolving the polymer, DMAc (Dimethylacetamide) and GBL (gamma-butyrolactone) purchased from Sigma-Aldrich were used. DMAc was used as a solvent to dissolve polymer at room temperature, and GBL was used as a solvent to dissolve polymer at high concentration. As a material for ATRP, the synthesis was carried out using CuBr (I) as a catalyst purchased and N, N, N', N'', N''-Pentamethyldiethylenetriamine (PMDETA) as a ligand from Sigma-Aldrich. As shown in Fig. 1 (c), Pentafluorostyrene which has many F functional group purchased from Sigma-Aldrich was used as a hydrophobic material for ATRP synthesis. Methanol, ethanol, and hexane purchased from SK Chemicals were used as a solvent for washing and drying the synthesized membrane. All materials were used without further purification.

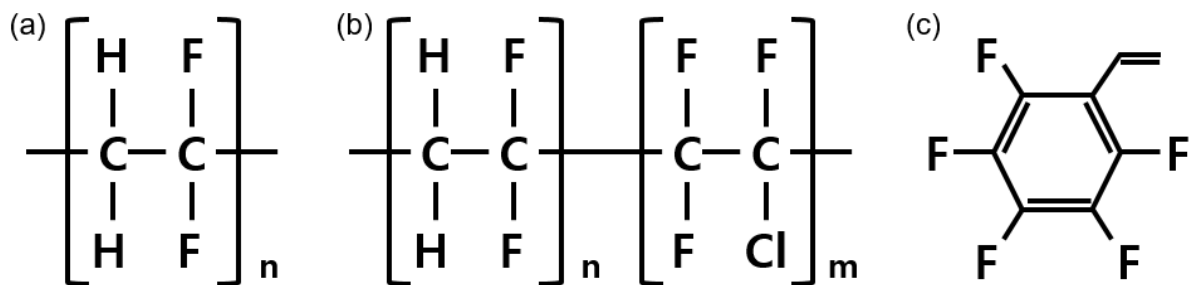


Fig. 1 Polymer for hollow fiber and ATRP reagent. (a) Polymer PVDF as a hollow fiber membrane, (b) Polymer PVDF-CTFE as a hollow fiber membrane, (c) Reagent pentafluorostyrene for chemical grafting.

II. Preparing for the experiment

2.1 ATRP for Synthesis of Hydrophobic Substance

Fig. 2 describe ATRP method, which was used as the method to attach the hydrophobic material to the polymer for hydrophobic enhancement. PVDF-CTFE can be reacted with a double bond of pentafluorostyrene to form a radical by removing Cl using a catalyst and a ligand. For synthesis, 45 g of PVDF-CTFE is mixed with 500 ml of DMAc and dissolved at 80 °C. After solution homogeneously melted and cooled to room temperature, 0.5 g of CuBr, 0.5 g of 4,4'-Dimethyl-2,2'-dipyridyl and 5 g of pentafluorostyrene are added together, and the temperature is raised to 80 °C. After the reaction is completed for setting time, remove the polymer and wash it several times with methanol to remove any remaining residual chemicals. Reacted polymer was soaked for 2 hours in ethanol, soaked in hexane for 2 hours subsequently, and dry at room temperature for 24 hours. The reaction time was 15, 20 and 25 hours.

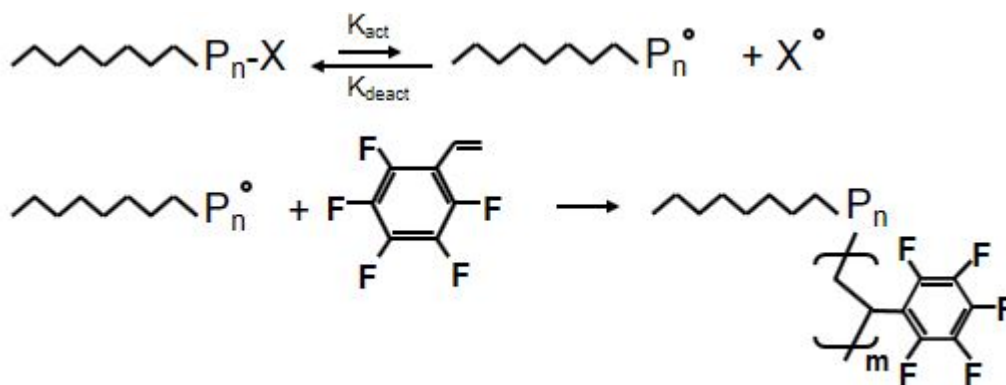


Fig. 2 Schematic diagram for ATRP method.

2.2 Hollow fiber spinning

To spin the hollow fiber for MD, a wet-jet spinning method to spun hollow fiber membrane. The spinning equipment for this is shown in Fig. 3. The spinneret used to spin the dual-layer hollow fiber has two inlets for the dope polymer solution. A PVDF-CTFE solution flows inward, and a PVDF solution flows outward. The conditions for the spinning were the same, and the spun hollow fibers were performed.

In the case of spinning, the experiment was carried out using two methods for increasing mechanical testing. In the case of NIPs, the polymer solution was maintained at room temperature. PVDF-CTFE

and PVDF are homogeneously dissolved in DMAc at room temperature. The prepared solution is purged with nitrogen at a pressure of 4 bars for 30 minutes by putting it in the dope tank of the spinning equipment of Fig. 3 (c). After the purging is completed, the pressure is adjusted to 2 bars. In the case of bore, as shown in Fig. 3 (a), pump (Fig. (b)) it constantly at 3 ml/min and flow it to the inside of the spinneret (Fig. (3)). In the case of coagulation baths (Fig. 3 (f)) was filled with tap water. Spun hollow fiber was collect in wind up bath (Fig. (h)) after pass through washing bath (Fig. (g)). After spun, hollow fibers were immersed in DI for 24 hours to remove residual solvent.

Another method is the TIPs method which uses the temperature difference between the polymer solution and the non-solvent. Unlike NIPs, TIPs spun with the temperature of 100 °C. In Fig. 3 (d), outer dope solution tank was maintained at 100 °C during spinning. All other conditions were the same as those of NIPs.

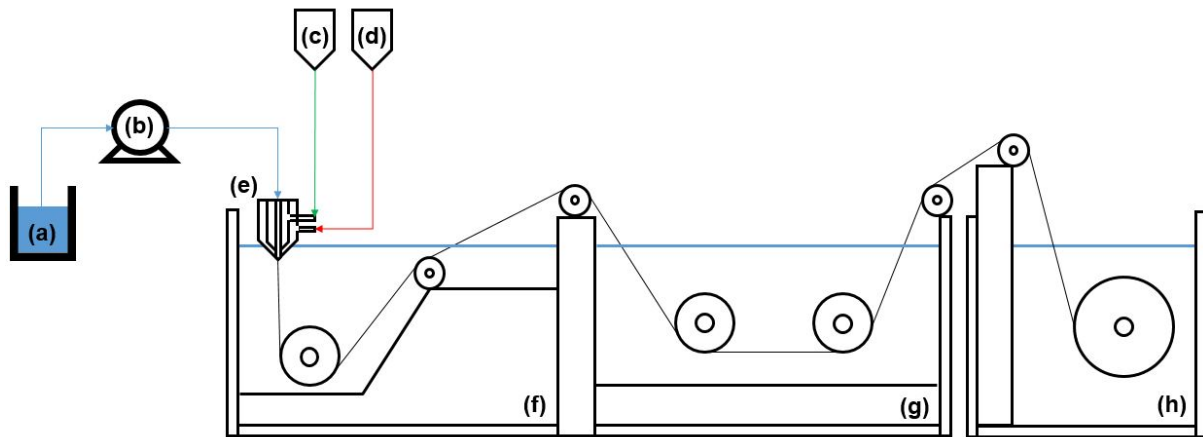


Fig. 3 Equipment for spinning. (a) Bore solution, (b) Pump for bore solution, (c) Inner dope solution tank, (d) Outer dope solution tank, (e) Triple-layer spinneret, (f) Coagulation bath, (g) Washing bath, (h) Wind up.

2.3 VMD

Spun membranes were immersed in ethanol for 2 hours, then simultaneously immerse in hexane for 2 hours. After immersing, take out the completely wet hollow fiber and dry at room temperature for 24 hours. The dry state of the membrane was confirmed by checking the peak of FTIR, and after confirmed there was no moisture peak, then the following experiment was conducted. Prepare the dried hollow fiber with a certain length to make the module. The module is prepared by inserting both ends of the hollow fiber into the tube and making the effective length to be 20 cm and filling the both ends with epoxy. Install the prepared module as shown in Fig. 4. The conditions were prepared as shown in Table. 1 and the performance of the prepared module was evaluated by VMD. DI filled the tank as a feed into

a hot water bath to keep it at 70 °C. The feed temperature flows into the hollow fiber’s lumen side at 100 ml/min using a peristaltic pump. When the vapor evaporated due to the vacuum passes through the pores of the membrane and condenses due to the cold trap and collects in the permeate tank, the flux is measured after a certain period.

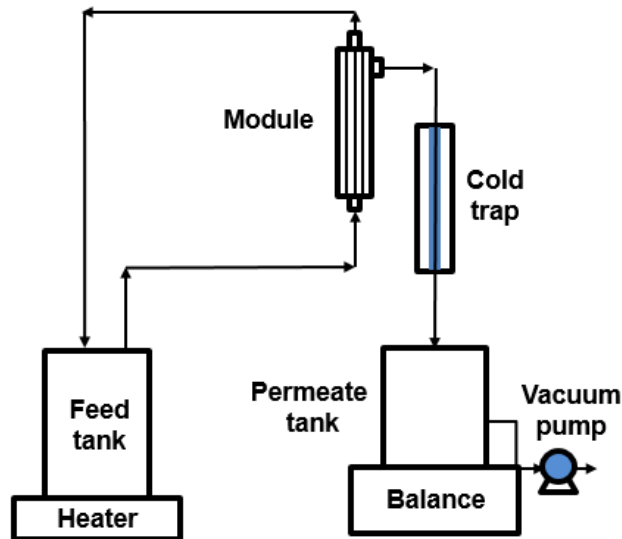


Fig. 4 Schematic diagram for VMD.

Table. 1 Conditions for VMD.

Feed	DI
Feed velocity (ml/min)	100
Feed temperature (°C)	70
Vacuum pressure (mbar)	25
Cold trap (°C)	0

III. Characteristic

3.1 Scanning electron microscopy (SEM)

S-4800 Hitachi devices were used to identify the cross-section of the hollow. To take the SEM, first, immerse the dried hollow fiber in liquid nitrogen and freeze rapidly. Hollow fibers were immersed in liquid nitrogen and broke for preparing cross-sectional images. After attaching the fractured section to

the holder, a platinum layer was spread on the surface of the cross-section to prepare a sample and take an image.

3.2 Attenuated total reflectance-Fourier transform infrared spectroscopy (ATR-FTIR)

The ATR-FTIR method using a Nicolet 6700 spectrometer (Thermo Scientific, USA) was used to confirm the results of chemical synthesis. Omnic 8.1 program was used as a program. Wave lengths of 600-4000 cm^{-1} were measured for 64 seconds per sample. The resolution used is 4 cm^{-1} .

3.3 Water contact angle

The contact angle was measured indirectly as a method for confirming the hydrophobicity of the surface. DI 5 μm was dropped onto the surface of the membrane through the sessile drop method. The contact angle was calculated by using the program, and the value was obtained. The samples were measured 10 times for each sample and averaged.

3.4 Measurement of Mechanical property

Tensile strength was measured to determine the mechanical strength of the spun hollow fiber. Universal Testing Instruments (Model AGS - 100 NX Shimadzu) was used as an equipment for measuring mechanical strength. The tensile strength was confirmed by pulling the hollow fiber prepared at 5 cm at a constant speed of 50 mm/min.

3.5 Viscosity measurement

It is important to find an appropriate viscosity for the polymer solution prepared for spinning hollow fibers. Viscometer (RVDF-II, BROOKFIELD, USA) was used to measure the viscosity of the polymer solution. The CP26 spindle was used and the speed was set at 10% and measured at room temperature.

3.6 Liquid Entrance Pressure (LEP)

As another method for measuring the hydrophobicity of the polymer, LEP was measured by applying pressure to push the solution into the membrane's pores and performing a wet test. Prepare 3.5 wt% NaCl and make a module with 20 cm, 5 hollow fibers for the test. The module was connected with equipment and put in DI water tank. As the pressure increases, the liquid fill with membrane's pore and

finally in DI salts were measured by conductivity changes. The pressure is increased from 0.2 bar. After holding for 10 minutes, confirm that there is no change in the conductivity, and then raise the 0.2 bar again until the conductivity changes. Repeat increasing and change conductivity, that point was measured as the LEP.

3.7 X-ray photoelectron spectra (XPS)

XPS were measured using a (Thermo Fisher, UK) system with a KAlpha (1486.6 eV) and a double-focusing hemispherical analyzer in order to identify the major chemical elements. The spot area is approximately 400 μm for each sample and the pass energy is 50 eV with the binding energy step size of 0.1 eV under the vacuum approximately 5×10^{-9} mbar. The high resolution was obtained with binding energy ranges 0.1 eV for analyzing the specific.

3.8 VMD Performance Evaluation

Water permeability was calculated to evaluate the performance of the spun hollow fiber membrane. The water permeability was calculated by using Equation (1) as the amount of evaporated water vapor condensed in the permeate tank.

$$J = V / (A * t) \quad (1)$$

Where: J : Permeate flux (LMH)
V : Permeate mass (kg)
A : Effective membrane area (m^2)
t : Time (hour)

3.9 Direct contact membrane distillation (DCMD) for evaluate wetting degree

The contact angle and LEP were measured to confirm the hydrophobicity of the modified membrane. However, experiments were conducted to confirm the effect of hydrophobicity and pore size on the practical application of MD. In the case of VMD, vacuum is applied to the outside of the membrane, so that even if the pore is wet and the feed solution comes out directly, it evaporates immediately and it is difficult to confirm the wetting. Therefore, DCMD was performed to confirm the wetting phenomenon in MD application. Experiments were conducted by adding isopropanol to accelerate the wetting of the membrane, considering that the running time was very long when only 3.5 wt% of NaCl solution was used as the feed solution. A solution of 3.5 wt% of NaCl and 20 wt% of IPA as feed was kept at 70°C and flowed at 100 ml/min. Permeate was maintained at room temperature using DI and flowed at a rate of 100 ml / min, which is the same as the feed. During DCMD, the feed is directed towards the lumen

side, and when the pore is wet, the salt is passed over to the permeate. We measured the conductivity of Permeate in real time and confirmed that the salt of the feed was passing. When the rejection decreased to less than 99.99 % as 25 mS/cm for the feed, the test was judged as wetting and the experiment was stopped.

Chapter 4. Results

I. Polymer selection

1.1 Background of PVDF-CTFE selection

In membrane distillation, the hydrophobicity of the membrane is important to prevent wetting phenomena. To prevent such wetting phenomenon, a polymer having a high hydrophobicity is used as membrane materials, and PVDF, PP, PVC, and PSf are usually used polymer. The hydrophobicity of various polymers was confirmed and compared using the contact angle measurement method which widely used as a method for measuring the hydrophobicity of such polymers.

First, a flat membrane is made to compare the contact angles of the polymers. Place the support layer on a glass plate and pour polymer solution on the support layer with a constant thickness of 150 μm using a casting knife. Place in an oven maintained at 100 $^{\circ}\text{C}$ and let the solvent evaporate for 1 hour. After 1 hour, the flat membrane was separated from the glass plate, and the contact angle was measured by the sessile drop method using the contact angle equipment. Fig. 5 shows the contact angle values.

As can be seen in Fig. 5, PP shows high hydrophobicity. This is a structure composed of only non-polar $-\text{CH}_2$, and because of this structure, it is possible to push water which has polar property. However, in the case of PP, ATRP, which is one of the chemical modification methods, can not be used since there is no applicable functional group.

As another example, it can be seen that PVDF, which is widely used, has high hydrophobicity. This is possible because it contains many functional group F, which is a strong hydrophobic atom. However, PVDF also has difficulty in accessibility because it does not have a functional group capable of modifying through ATRP. Fig. 6 shows the results after combining various polymers with styrene through ATRP modification. As shown in Fig. 6 (a), PVDF shows no change in the peak after the reaction.

Also, in the case of widely used PVC, the hydrophobicity is relatively low compared to PVDF or PP. However, the Cl functional group in the PVC reacts with the ligand and the catalyst easily and then form a radical site, which allows chemical bonding with other hydrophobic materials. As shown in Fig. 6 (b), it is possible to confirm the change of peak due to grafting with styrene. It can be seen that the peak of $\text{C}=\text{C}$ bond which does not exist in PVC appears after reacting with styrene after ATRP. It can be seen that the $\text{C}=\text{C}$ bond present in the styrene substitutes for the Cl position of PVC and peaks appear.

Finally, when PVDF-CTFE is examined, it can be seen that it has a relatively higher contact angle value than PVDF and PVC though it is lower than PP as shown in Fig. 5. This is because the polymer contains a large amount of F, which is a hydrophobic atom, as compared with other polymers. Also, the Cl functional group in PVDF-CTFE has the advantage of being able to bind with other chemicals through the ATRP method like PVC. In the case of PVDF-CTFE as well as PVC, peaks appear along the styrene at around 1600 cm^{-1} after the synthesis. This 1600 cm^{-1} fraction also shows the C=C bond peak of styrene as well as PVDF, indicating that the Cl functional group of PVDF-CTFE detached after ATRP and that styrene was successfully reacted.

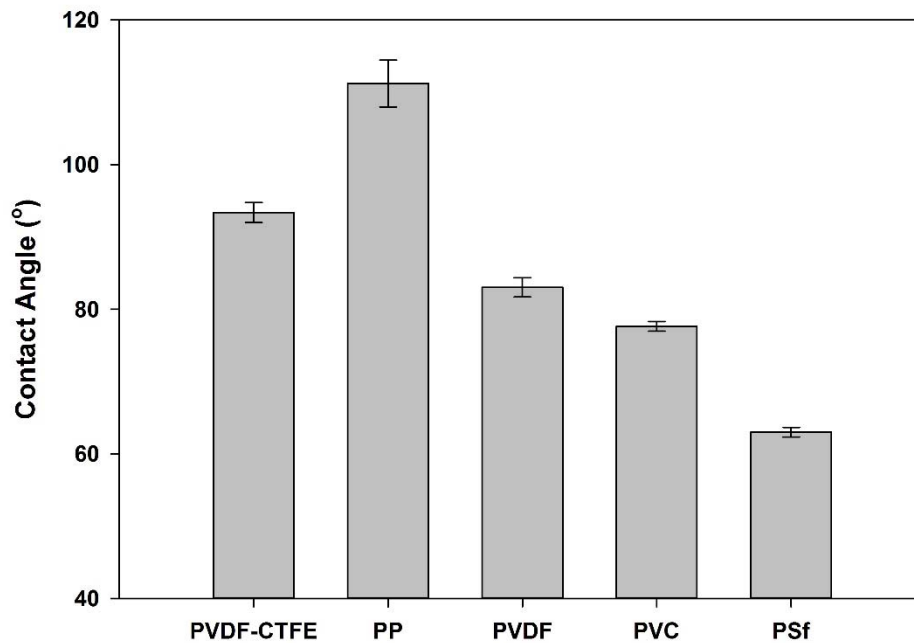


Fig. 5 Comparison of contact angle value with various polymers.

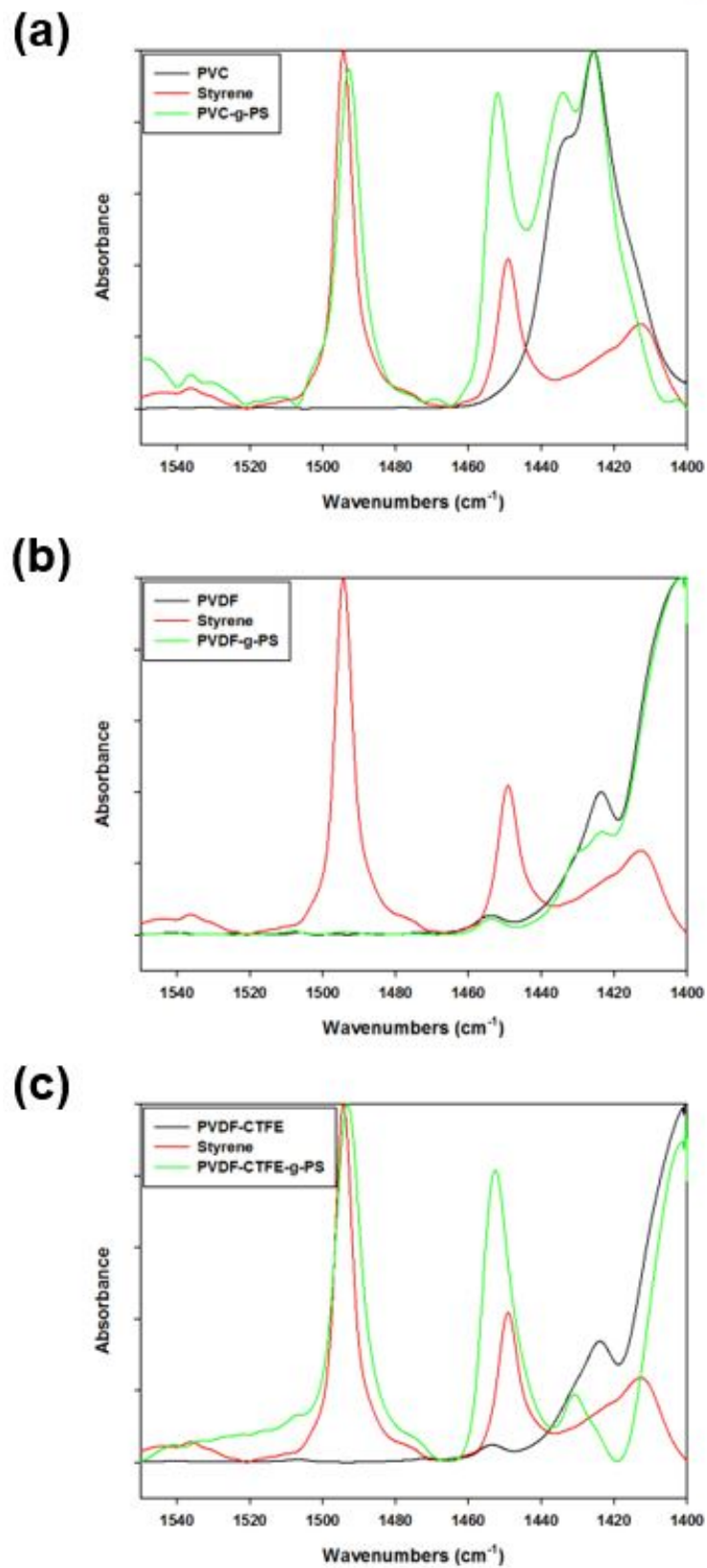


Fig. 6 ATRP changes checked by FTIR for several polymers. (a) PVC with styrene, (b) PVDF with styrene, (c) PVDF-CTEF with styrene.

1.2 Single-layer hollow fiber spinning

Experiments were conducted to compare the performance of PVDF-CTFE with that of PVDF, a widely used polymer. First, the concentration of the polymer solution was selected for comparison by spun a single-layer membrane. Since the viscosity of two polymers differs when they are dissolved in the same solvent, the viscosities are compared at different concentrations. In the case of PVDF-CTFE, it was confirmed that the viscosity was lower than that of PVDF even at the high concentration. Because of this difference, the solution was prepared by different concentration but same viscosity. Table. 2 shows the conditions of the solution prepared for this purpose. In the case of PVDF, concentrations of 15, 17, and 19 wt%, which are commonly used in other articles, were selected and dissolved homogeneously in DMAc for 24 hours at room temperature. In the case of PVDF-CTFE, since the viscosity is low at the same concentration compare with PVDF, a higher concentration was selected. 26, 28 and 30 wt% were selected, and the solution was prepared by the same method as PVDF to measure the viscosity.

Table. 2 Comparison of viscosity at different polymer concentration.

		Concentration (wt%)	Viscosity (cP)
Polymer	PVDF	15	2215
		17	4600
		19	8977
	PVDF-CTFE	26	2178
		28	4616
		30	9055
Solvent	DMAc		
Temperature (°C)	25		

As shown in Fig. 7, the PVDF 15 wt% and PVDF-CTFE 26 wt%, 17 wt% and 28 wt%, and 19 wt%

and 30 wt%, respectively, showed similar viscosities. Based on these results, the experiment was conducted by selecting 17 wt% for PVDF and 28 wt% for PVDF-CTFE. In the case of 15 wt% of PVDF and 26 wt% of PVDF-CTFE, it is not suitable for spinning because of low viscosity. In the case of 19 wt% and 30 wt%, it is possible to fabricate. However, considering high concentration decreases flux because hollow fiber made with dense structure, PVDF, 17 wt % and 28 wt% for PVDF-CTFE were not chosen.

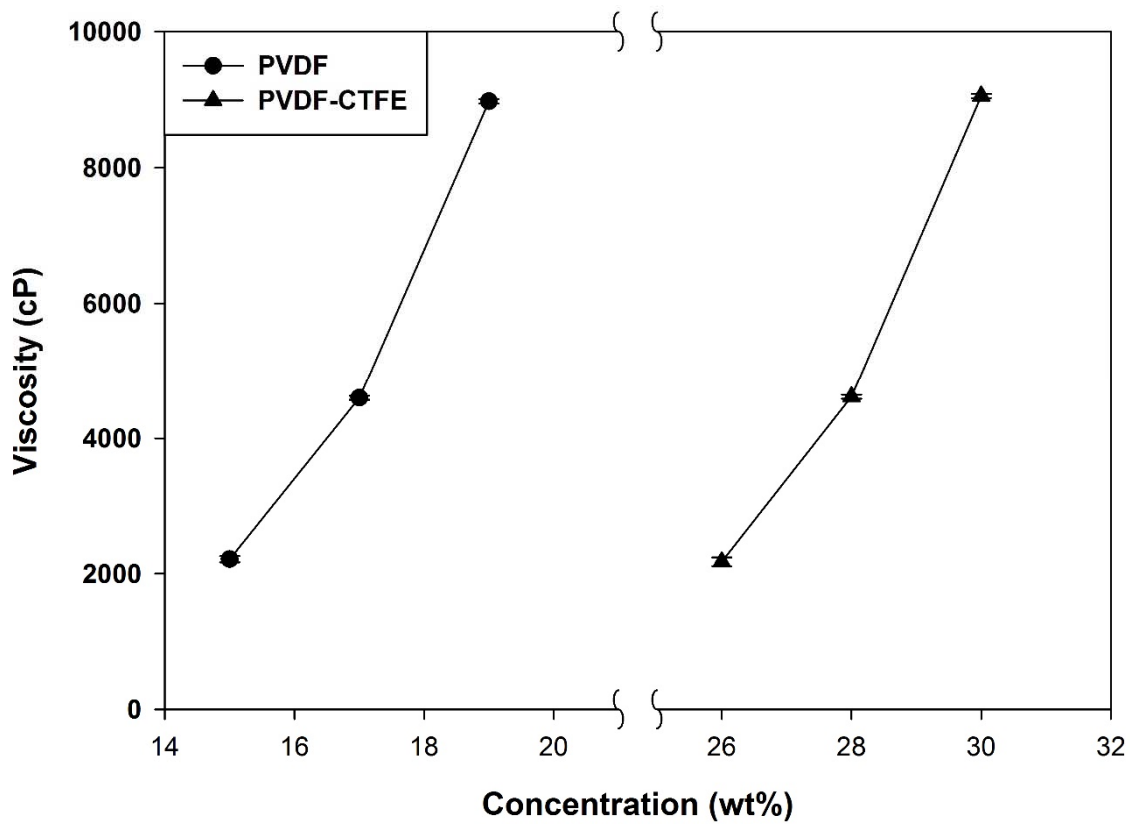


Fig. 7 Comparison of dope polymer solution's viscosity at each concentration.

A single-layer hollow fiber was spun in each of these solutions under the condition as shown in Table.

3. The hollow fibers were spun using the equipment shown in Fig. 3. To remove the air bubbles trapped in the dope solution, before the spinning, the tank containing the dope solution was kept at the pressure of 4 bars for 30 minutes. After that, nitrogen was removed, and pressure was applied to spun. At this time, the spinning conditions were the same as the pressure, bore type, and bore speed of the two cases as shown in Table. 3. After spinning, it is necessary to dry the hollow fibers to analyze the characteristics. The spun membranes were soaked in ethanol for 2 hours. Then just dipped in hexane directly and held for 2 hours. The hollow fibers are then removed from the hexane and keep at room temperature for 12 hours to dry naturally. To confirm that the membrane's drying condition, the lumen side and the shell side of the hollow fiber were checked with FTIR to confirm that there was no moisture peak, and the following experiment was conducted.

Table. 3 Spinning conditions for dual-layer hollow fiber.

Dope	PVDF-CTFE
	PVDF
Dope pressure (bar)	1
Bore	DI
Bore flow rate (ml/min)	3
Outer coagulant	Tap water
Air gap (cm)	3
Dope temperature (°C)	25

To characterize the dried membrane, the cross-section was confirmed by SEM to confirm the structure of the pore, and tensile strength, elongation at break and young's modulus were measured to measure the mechanical strength of the membrane. Finally, to measure the performance of the membrane, VMD method was conducted, and the equipment was set up as shown in Fig. 4.

Before measuring SEM images, to measure the cross-section with SEM, put the dried hollow fiber membrane in liquid nitrogen for a sufficient time and break the hollow fiber. The fractured section was confirmed by SEM. As can be seen in Fig. 8, PVDF has the same shape of finger-like structure both inside and outside. This is because the inside and outside are all in direct contact with water so that instantaneous demixing occurs and a large finger-like structure is formed due to the rapid exchange of solvent and water. It can be seen that the sponge-like structure is thickly formed in the middle part. This can be seen as the structure of the pore is made small because the solvent does not reach directly and the solvent is gradually released.

However, in the case of PVDF-CTFE, PVDF-CTFE has a finger-like structure in outside of hollow fiber similar to that of PVDF, but the inside of the PVDF-CTFE has very large macrovoids. The solution can be seen as a large pore that comes out of the solvent quickly as it comes in contact with water. In the case of the inner side about the outer side, since the contact is made with water as soon as possible, it is confirmed that this structure is formed as the solvent exchanges more rapidly before the solution hardens. It can also be seen that the sponge-like structure in the middle part is relatively thinner than PVDF due to the large macrovoids structure created by this rapid exchange of solvent and non-solvent. It was confirmed that the inside of the PVDF and the PVDF-CTFE hollow fiber had different structures even though the inside and outside were spun with water.

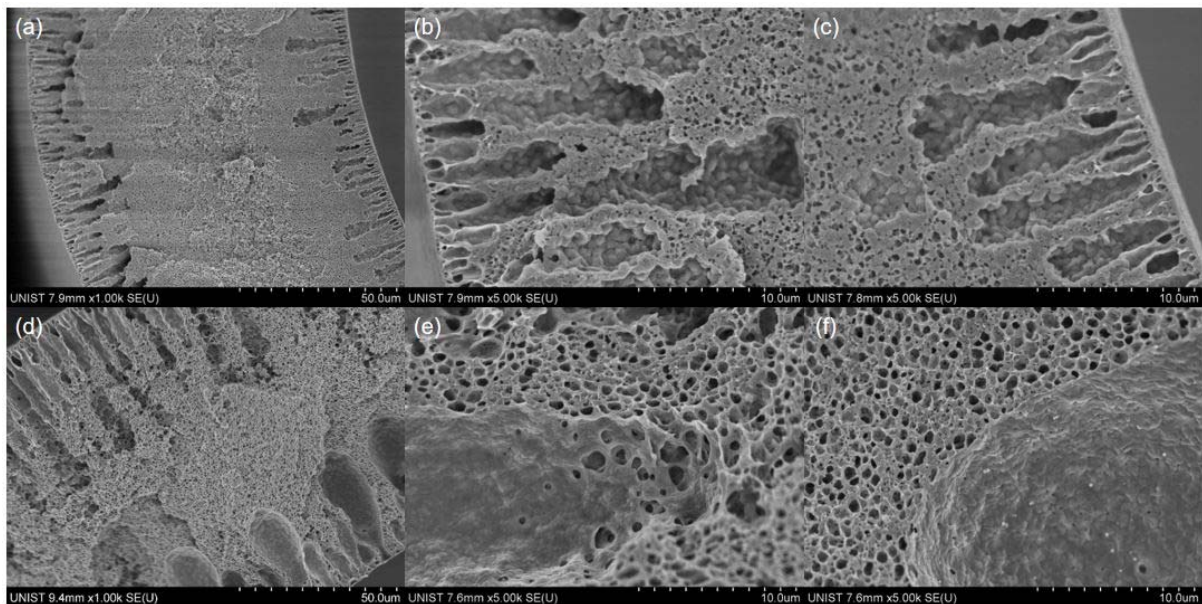


Fig. 8 Cross-sectional images for single-layer hollow fibers. (a) PVDF 17 wt% cross-section, (b) PVDF shell side, (c) PVDF lumen side, (d) PVDF-CTFE 28 wt% cross-section, (e) PVDF-CTFE shell side, (f) PVDF-CTFE lumen side.

1.3 Measurement of tensile strength and VMD flux

The tensile strength, elongation, and Young's modulus were measured to compare the mechanical strength of the single-layer membrane. To measure this, first, the dried hollow fiber's mechanical strength was measured through the instrument at a constant rate with 3 cm, and both ends were pulled at a constant speed to measure the respective values. At this time, the pulling speed of the hollow fiber was set to 50 mm/min, and the experiment was performed 10 times each. As can be seen in Table. 4, the thickness of PVDF is relatively thinner than that of PVDF-CTFE, but it has higher tensile strength. Also, it can be seen that the stretched length is shorter than that of PVDF-CTFE, but the Young's modulus obtained by calculation is much higher than that of PVDF-CTFE. In the case of PVDF-CTFE, the elongation length is measured long until it is broken, but the value of tensile strength and Young's modulus is small. This can be explained in conjunction with the result of checking the section through the SEM. The thick macrovoids layer is formed on the inner side, and the outer side is also thickly formed on the finger-like structure so that the sponge-like structure is thinly formed in the middle part, so that it has a low mechanical strength even though it spun at a higher concentration of PVDF. As a result, PVDF-CTFE has a higher concentration than PVDF but has a low mechanical strength, which indicates that the membrane cannot withstand a high pressure when the VMD test is performed.

Table. 4 Comparison of single-layer hollow fiber's mechanical strength.

	Thickness (μm)	Stress (N/mm^2)	Elongation at break (%)	Young's modulus (MPa)
PVDF	106.6 (9.28)	3.36 (0.103)	150.4 (11.77)	64.07 (5.93)
PVDF-CTFE	132 (7.26)	2.102 (0.068)	487 (12.11)	4.77 (0.0952)

*In case of Young's modulus, calculate with 0.5 ~ 1 % of strain

*() is error value

In addition to the above results, VMD experiments were conducted to evaluate the performance of each membrane. The experimental conditions of all the membranes were the same as shown in Table 4.

For the VMD experiment, prepare the dried hollow fiber so that the effective length is 20 cm, and insert 5 numbers of hollow fibers into the module. Then, both ends are covered with epoxy. After the epoxy has hardened, cut the cross-section of the hollow fiber. Prepare this module by connecting it to the installed VMD device as shown in Fig. 4.

As a condition of the experiment, DI is maintained at a constant temperature of 70 °C in the case of the feed by circulating through the lumen side of the hollow fibers using a peristaltic pump at a rate of 100 ml/min. At the same time, a vacuum pump is used to keep the vacuum at 50 mbar on the shell side of hollow fibers. This vacuum pressure on the shell side as a driving force to evaporate the feed solution. As a result, the evaporated water collected in the coagulation bath was used for the flux calculation.

As Fig. 9 shown, PVDF-CTFE has higher flux than PVDF. This is because it has a relatively thin sponge-like structure. Also, it was confirmed that the same tendency could be obtained as the SEM results show that the evaporated water due to the thick macrovoid is easily permeated through the cross-section.

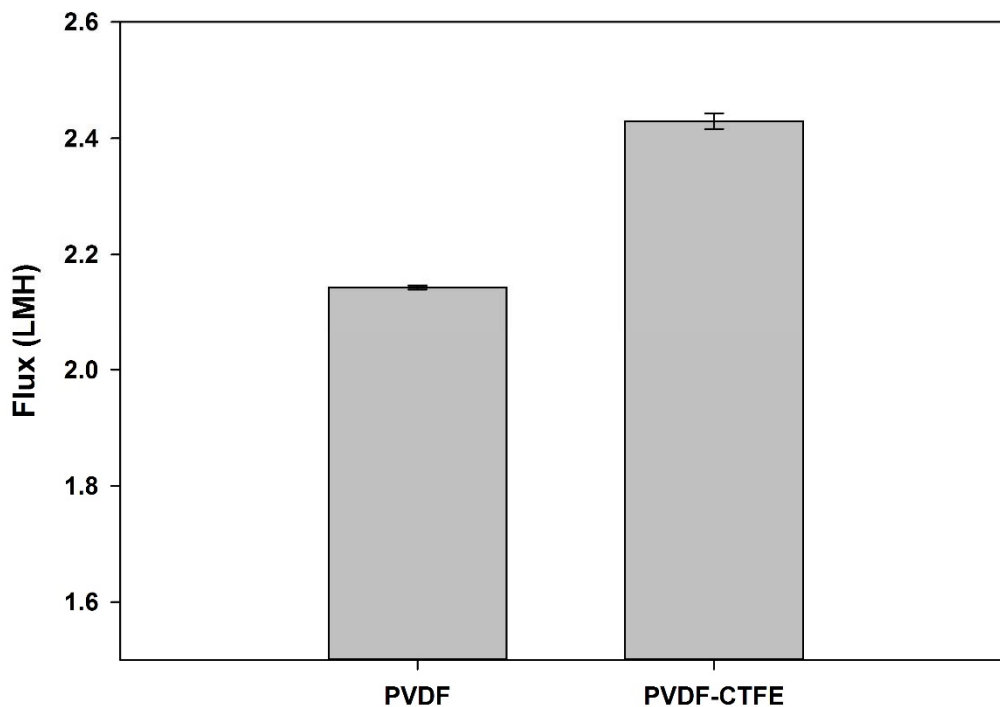


Fig. 9 Comparison of VMD flux for each single-layer hollow fiber.

In addition, LEP experiments were conducted to confirm hydrophobicity, an important factor for preventing wetting phenomenon. The experiment was carried out using 3.5 wt% NaCl. As can be seen in Fig. 10, PVDF-CTFE shows lower LEP value even though it is more hydrophobic than PVDF. As can be seen in Fig. 8, it can be seen that the solution easily penetrated due to the existence of macrovoids inside.

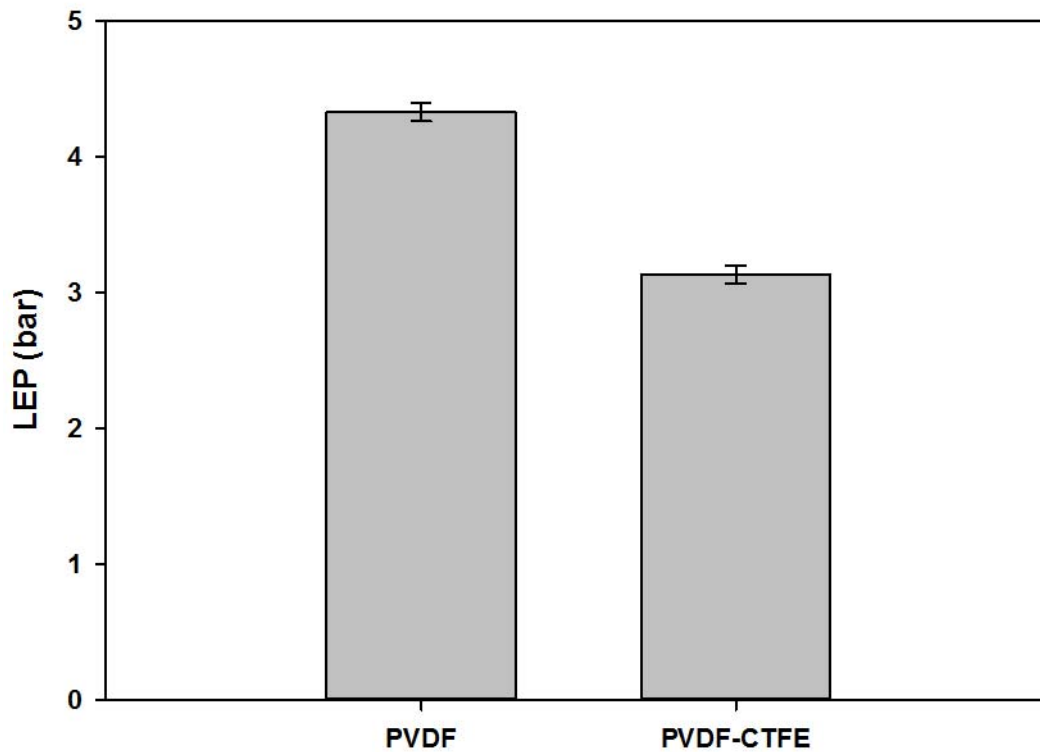


Fig. 10 Comparison of each hollow fiber's LEP.

Previous experiments have shown that PVDF-CTFE has higher flux values than PVDF in VMD and applies to MD. This can be confirmed as a result of the formation of a thick macrovoids structure and the thin sponge-like structure in exchange for solvent when spun relatively faster than PVDF. However, the PVDF-CTFE membrane needs to be improved to solve the problem of not being able to withstand high pressure due to its weak mechanical strength and large macrovoids. For this purpose, the following experiment was conducted to increase the mechanical strength of the membrane.

II. Spinning for Strength Improvement

To improve the mechanical strength of PVDF-CTFE, two methods have been selected and tested. First, two layers of the solution are used to spun a dual-layer hollow fiber. This is a method in which two solutions are divided into inner and outer portions and simultaneously spun. In this case, the outer solution serves as a support layer and the inner part serves as an active layer as a porous structure. At this time, the PVDF layer as a support has an advantage that the mechanical strength can be increased. Another method is to increase the strength of the hollow fiber due to its high concentration, which requires a high temperature to dissolve the high concentration of polymer. The TIPs method can be used as a method of making a hollow fiber at such a high concentration and a high temperature. Experiments were conducted to increase the mechanical strength through these two methods

2.1 Spinning dual-layer hollow fibers

The PVDF-CTFE solution was used as the solution when spinning the dual-layer hollow fiber membrane. Outside, PVDF solution with high mechanical strength was spun with PVDF-CTFE so that it could act as a support layer. The concentration of the solution was determined to be 17% by concentration of PVDF and 28% by concentration of PVDF-CTFE which have the same viscosity as same as single-layer membrane. The spinning conditions were the same as when spinning single-layer hollow fiber. The dope solution, the bore solution speed, and air gap are same as single-layer spinning. Table. 5 shows the spinning conditions.

Table. 5 Conditions for spinning dual-layer hollow fiber.

Dope (wt%)	Inner	PVDF-CTFE	28
	Outer	PVDF	17
Dope pressure (bar)	Inner	1	
	Outer		
Bore solution	DI		
Bore flow rate (ml/min)	3		
Outer coagulant	Tap water		
Air gap (cm)	3		
Dope temperature (°C)	25		

The dried membrane was dried using the same method as in the previous method, and the SEM was also taken in the same method to check pore structure. As can be seen from Fig. 11, the inside of dual-layer hollow fiber's cross-section is composed of the macrovoids, just like the lumen of the PVDF-CTFE single-layer membrane. Also, it can be seen that the end of the PVDF-CTFE layer has a thin sponge-like structure in the case of a dual-layer membrane, compared to a finger-like structure in the case of a single-layer membrane. This is because the PVDF-CTFE solution is surrounded by a PVDF solution and the outer side is in contact with the solution which is DMAc. Instead of the finger-like structure, the PVDF solution causes slow demixing due to the solvent and generate thin sponge-like structure layer. The exchange of PVDF-CTFE solvent with that of the inner bore solution occurs

sufficiently, and it can be confirmed that a thick macrovoids structure can be formed. On the outer side, it can be seen that the PVDF is in direct contact with water and forms a thick finger-like structure. The PVDF solution also shows that the sponge-like structure of the inner side is thinner than the finger-like structure. Similar to PVDF-CTFE solution, there is no direct exchange between solvent and non-solvent so that no finger-like structure is formed and a thin sponge-like structure is formed at the interface.

It was confirmed that the structure of the PVDF-CTFE layer was formed thick macrovoids structure and that the shell side had thick finger-like structure which is the PVDF layer. Also, in the case of the point where the two solutions meet, it is confirmed that a thin sponge-like structure is formed because the solution and the solution which is used same solvent meet and thus the solvent is not directly exchanged each other.

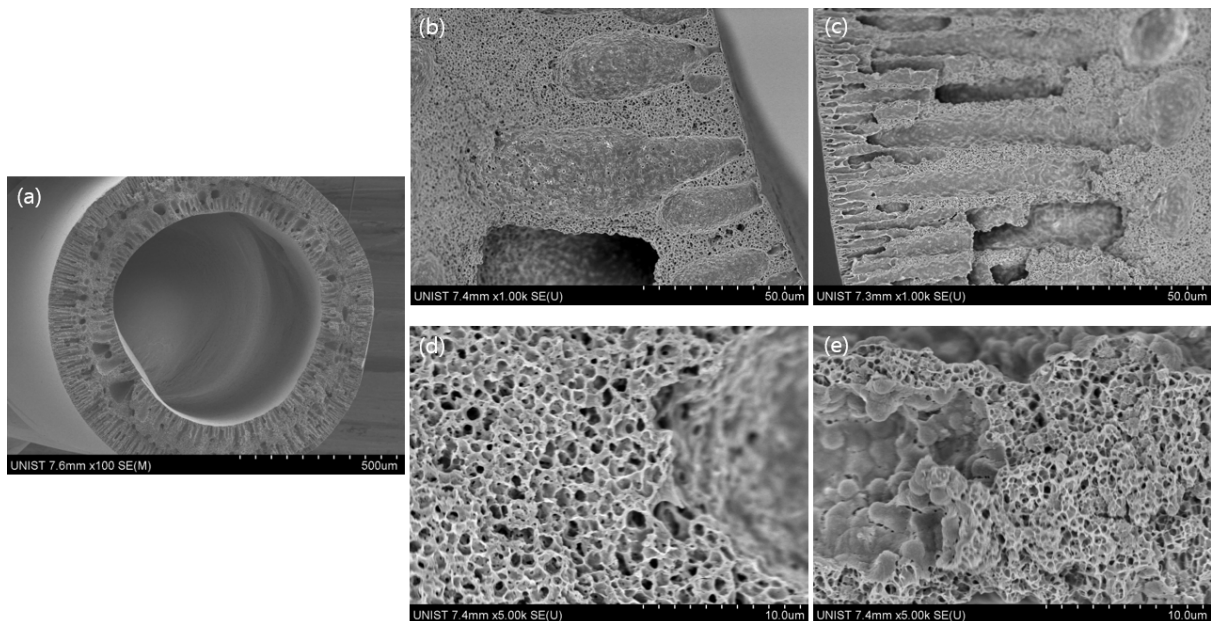


Fig. 11 Cross-sectional images for dual-layer hollow fiber. (a) Dual-layer cross-section, (b) Lumen side of hollow fiber which is PVDF-CTFE, (c) Shell side of hollow fiber which is PVDF, (d) Lumen side of hollow fiber which is PVDF-CTFE, (e) Shell side of hollow fiber which is PVDF.

To analyze the characteristics using the dried membrane, mechanical strength was first measured. As measuring single-layer hollow fiber, the tensile strength was measured 10 times with 3 cm of hollow fibers. As Table. 6 shown, it can be seen that the thickness becomes thicker in comparison with the

single-layer hollow fiber. The tensile strength, strain, and Young's modulus were become similar to those of PVDF. The elongation at break was reduced when compared with that of the PVDF-CTFE single-layer membrane, but the tensile strength and the Young's modulus were enhanced to a value similar to that of the PVDF single-layer membrane. It can be seen that the PVDF is acted on the inside as a support and the mechanical strength is increased.

Table. 6 Comparison of mechanical strength for single and dual-layer hollow fibers.

	Thickness (μm)	Stress (N/mm^2)	Elongation at break (%)	Young's modulus (MPa)
PVDF	106.6 (9.28)	3.36 (0.103)	150.4 (11.8)	64.07 (5.93)
PVDF- CTFE	132 (7.26)	2.10 (0.068)	487 (12.1)	4.77 (0.0952)
Dual	200 (14.4)	2.81 (0.086)	77.9 (2.84)	62.5 (3.25)

*In case of Young's modulus, calculate with 0.5 ~ 1 % of strain

*() is error value

The flux through the VMD was also compared with that of the single-layer hollow fibers. Like measure

in the previous, the module was prepared hollow fibers as 20 cm of the effective length. The flux was measured by VMD, and the result was shown in Fig. 12. At this time, it can be confirmed that the membrane has a higher flux than the single-layer membrane even though the membrane is thick. It can be confirmed that the sponge-like structure layer is relatively thin compared to the single-layer membrane at the part where the two solutions meet. The macrovoids structure at the inner part and the finger-like structure at the outer part were contributed increasing flux.

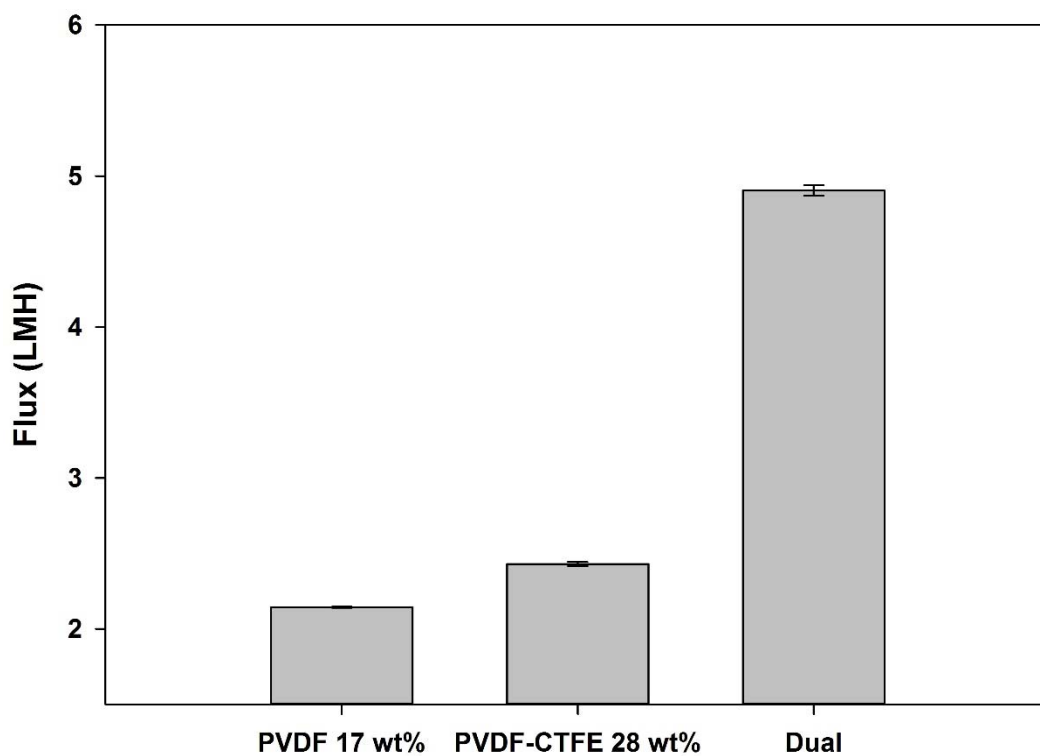


Fig. 12 Comparison of VMD flux for single & dual-layer hollow fibers.

Improvement of flux was confirmed through VMD. Furthermore, the LEP experiment was conducted

to confirm the unsecured wetting phenomenon. As can be seen in Fig. 13, it still shows lower values than PVDF but higher values than PVDF-CTFE. It can be seen that the PVDF-CTFE layer still has a large macrovoid but the wetting phenomenon can be prevented due to the thickening of the membrane due to the dual-layer structure.

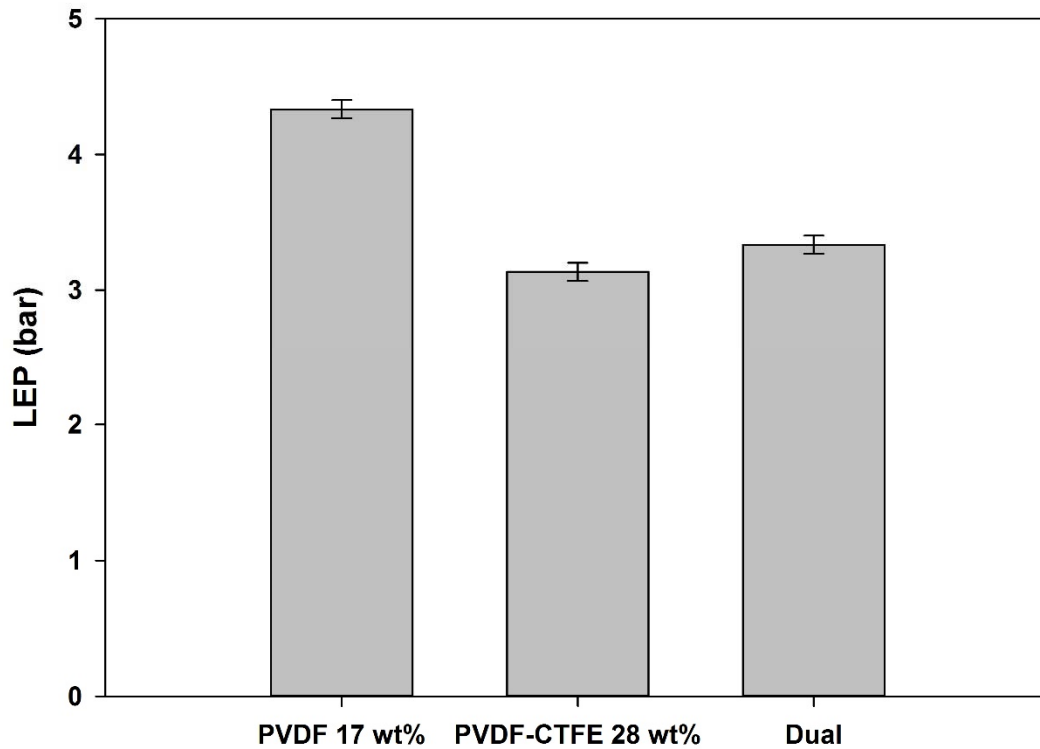


Fig. 13 Comparison of LEP which affect to hydrophobicity.

2.2 Spinning through the TIPs method

As a method of increasing the temperature of the solution for spinning, it is possible to dissolve more high concentration of polymer in a solvent. For this purpose, GBL was used as a solvent different from the solvent used previously. Because TIPs spun hollow fibers at high temperatures, it is necessary to use a poor solvent, which does not dissolve the polymer at low temperatures but can dissolve the polymer at high temperatures. Conditions for TIPs emission are shown in Table. 7. As can be seen here, it was confirmed that the higher the concentration, the higher the viscosity. Radiation was prepared with a selected concentration of the solution.

Before spinning, the polymer was dissolved by stirring at high temperature for 24 hours to dissolve the polymer in the solvent homogeneously. The spinning apparatus was the same apparatus as shown in Fig. 14, and the line which the dope solution is passing was covered with a heating tape so that the solution's temperature can be maintained. The viscosity of each solution was measured while maintaining the temperature at 100 °C. In the case of 45 wt%, the spinning was not proceeded due to too high viscosity, so that the subsequent experiments were carried out with only 35 and 40 wt% hollow fibers.

Table. 7 Conditions for spinning with TIPs method.

Polymer	PVDF-CTFE		
Concentration (wt%)	28	35	40
Viscosity (cP)	4616	11967	27144
Dope pressure (bar)	1		
Bore solution	DI		
Bore flow rate (ml/min)	3		
Outer coagulant	Tap water		
Air gap (cm)	3		
Dope temperature (°C)	100		

Spinning was carried out with the previously prepared solution. As for spinning conditions, spinning was carried out by preparing doping pressure, bore type, bore speed, air gap, and coagulation bath as tap water as shown in Table. 7. The hollow fiber thus obtained was dried by the same method as above, and the structure of the cross-section was confirmed by SEM. The cross-sectional images according to each concentration are shown in Fig. 14. As can be seen in the Fig. 14, it can be seen that the visual pores in the case of 35 wt% of Fig. 14 (b) and the outer sponge-like structure layer are absent compared to the 28 wt% of Fig. 14 (a) and the dense structure is formed. Also, it can be seen that the cross-section in which the 40 wt% solution is radiated forms a dense structure as a whole in the case of Fig. 14 (c). This shows that the higher the polymer concentration, the more the mechanical strength is increased.

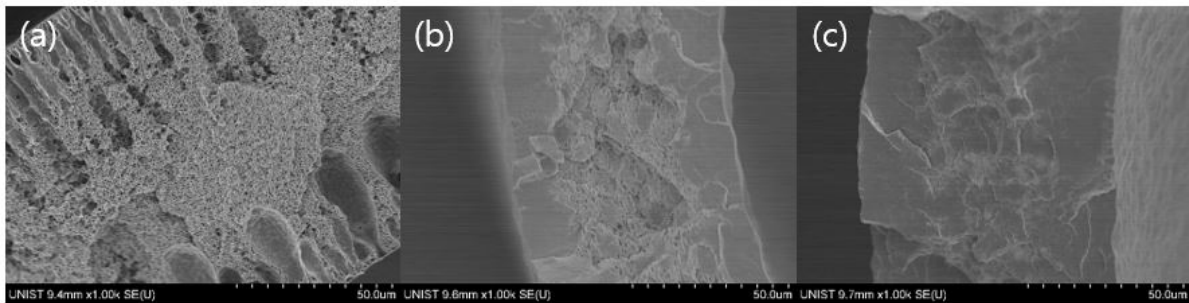


Fig. 14 Cross-sectional images for TIPs. (a) 28 wt% of PVDF-CTFE, (b) 35 wt% of PVDF-CTFE, (c) 40 wt% of PVDF-CTFE.

Experiments were also conducted to confirm the enhancement of mechanical strength. As shown in Table. 8, when the results of the tensile strength test are confirmed, the values of stress, elongation at break, and young's modulus increase as the concentration increases. It can be confirmed that a polymer having a high concentration is homogeneously dissolved in a solvent and is emitted into a hollow fiber form to form a uniform structure, thereby forming a more robust structure. In the case of the prior dual-layer structure, the tensile strength is higher than that of pure PVDF, even though the thickness is thinner when spinning with TIPs.

Table. 8 Comparison of mechanical strength for single-layer hollow fibers spun with TIPs method.

Concentration (wt%)	Thickness (μm)	Stress (N/mm^2)	Elongation at break (%)	Young's modulus (MPa)
28	132 (7.26)	2.10 (0.068)	487 (12.11)	4.77 (0.0952)
35	75.4 (2.84)	5.64 (0.545)	1440 (53.2)	4.78 (0.146)
40	80.8 (4.54)	10.27 (0.768)	1800 (19.0)	7.12 (7.25)

*In case of Young's modulus, calculate with 0.5 ~ 1 % of strain

*() is error value

The membranes spun by TIPs were dried and prepared in the same method as the previous. Fig. 15 shows that the 35 wt% and 40 wt% showed a much reduced flux compared to 28 wt%. As can be seen from the SEM, it can be seen that the evaporated water vapor becomes difficult to pass through due to the dense structure, and the flux decreases accordingly.

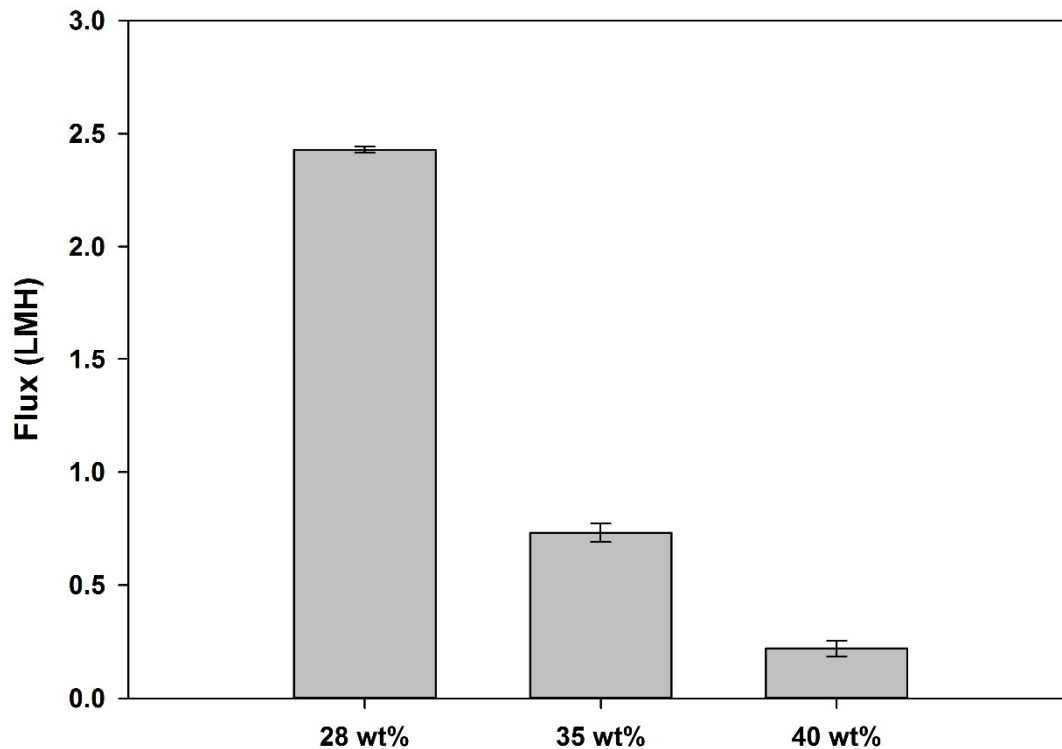


Fig. 15 VMD flux comparison for TIPs hollow fibers which spun at different polymer concentration.

Previously, the hollow fiber was formed through PVDF-CTFE, which has high hydrophobicity, and performance evaluation was conducted through VMD. When the cross-section was confirmed, it was confirmed that the structure had a higher flux due to the existence of macrovoids. However, the experiment was conducted to solve the problem that the mechanical strength is low and it can not withstand high pressure. As a support, two methods were used as a membrane spinning method. When TIPs method was used, the tensile strength was increased, but the flux was considerably deteriorated. However, in the case of the dual-layer hollow fiber membrane, it has a tensile strength similar to that of the PVDF single-layer membrane, and it has a high flux because it has a thin sponge-like layer and a

thick macrovoids. Based on this, hydrophobicity enhancement experiment was carried out to prevent wet phenomenon which is an important problem of MD through a dual-layer hollow fiber membrane.

III. Spinning dual-layer hollow fibers for enhancement of hydrophobicity

Two methods are used to further improve the hydrophobicity of the spun hollow fibers. It is easy to blend a hydrophobic material to the dope solution. As a representative hydrophobic material, PTFE is used to increase the hydrophobicity and confirm the flux change. Secondly, the hydrophobicity enhancement was experimented by analyzing the change of the flux by increasing the hydrophobicity of the polymer by binding the hydrophobic reagent through the chemical bond.

3.1 Improving hydrophobicity through blending PTFE as an additive

Through the blending, hydrophobic PTFE was selected as a method of improving the hydrophobicity by changing the hydrophobicity of the hollow fiber by mixing the hydrophobic material with the dope solution for spinning. The experiment was carried out by mixing PTFE in PVDF-CTFE solution directly to the feed solution. First, we investigated the change of contact angle according to the concentration of PTFE. At this time, when preparing the solution, mix PTFE with 20, 40, 60, 80 wt% of PVDF-CTFE. The solution is prepared by stirring for 24 hours. After that, we prepared a flat membrane prepared for the contact angle measurement. In order to confirm that PTFE is mixed properly in the prepared flat membrane, it was evaluated by peak analysis through FTIR and hydrophobicity increase by contact angle and LEP.

First, as shown in Fig. 16, the peak of PVDF-CTFE decreases and the peak of PTFE increases with the content of PTFE. It can be seen that the peaks decrease at 1400 cm^{-1} , 840 cm^{-1} and 870 cm^{-1} , which can be confirmed by pure PVDF-CTFE peaks. In addition, 1200 cm^{-1} and 1160 cm^{-1} peaks increased with PTFE content. It is also confirmed that PTFE is well mixed to form a flat membrane.

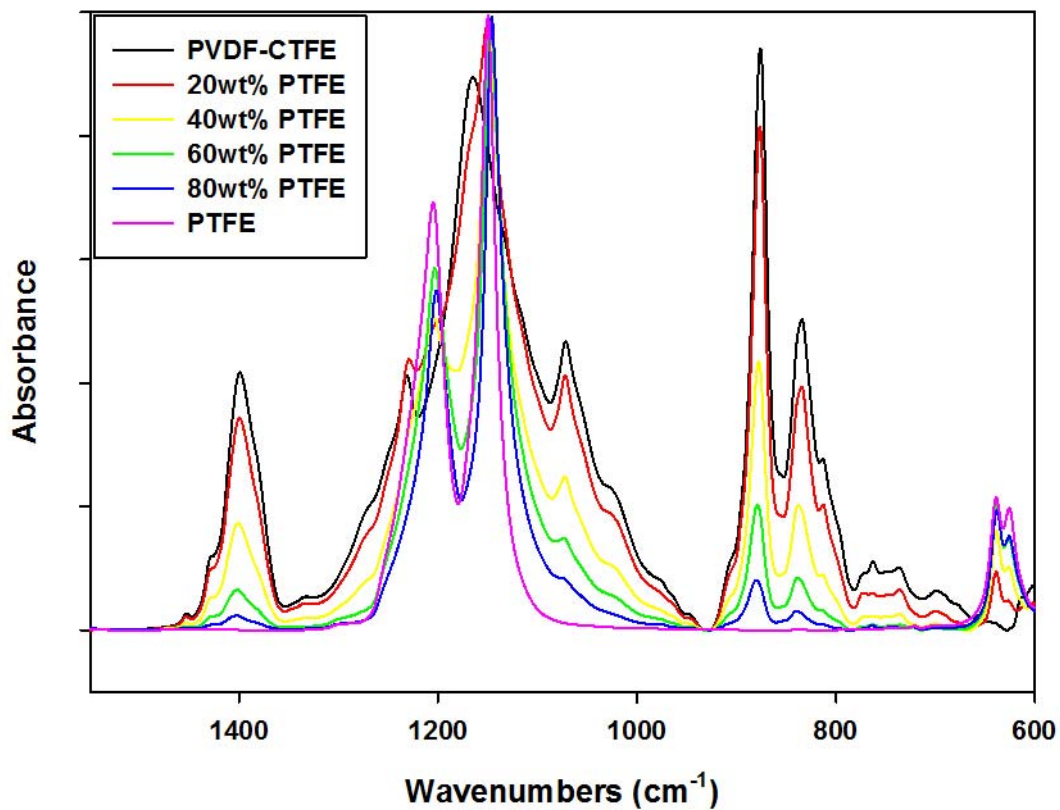


Fig. 16 FTIR peak comparison with different concentration of PTFE.

In addition, the hydrophobicity increases with the PTFE content through the contact angle as shown in Fig. 17. It can be seen that the hydrophobic property of PTFE is increased and added to PVDF-CTFE. However, it was confirmed that the higher the PTFE content, the lower the viscosity of the solution and affect the radiation.

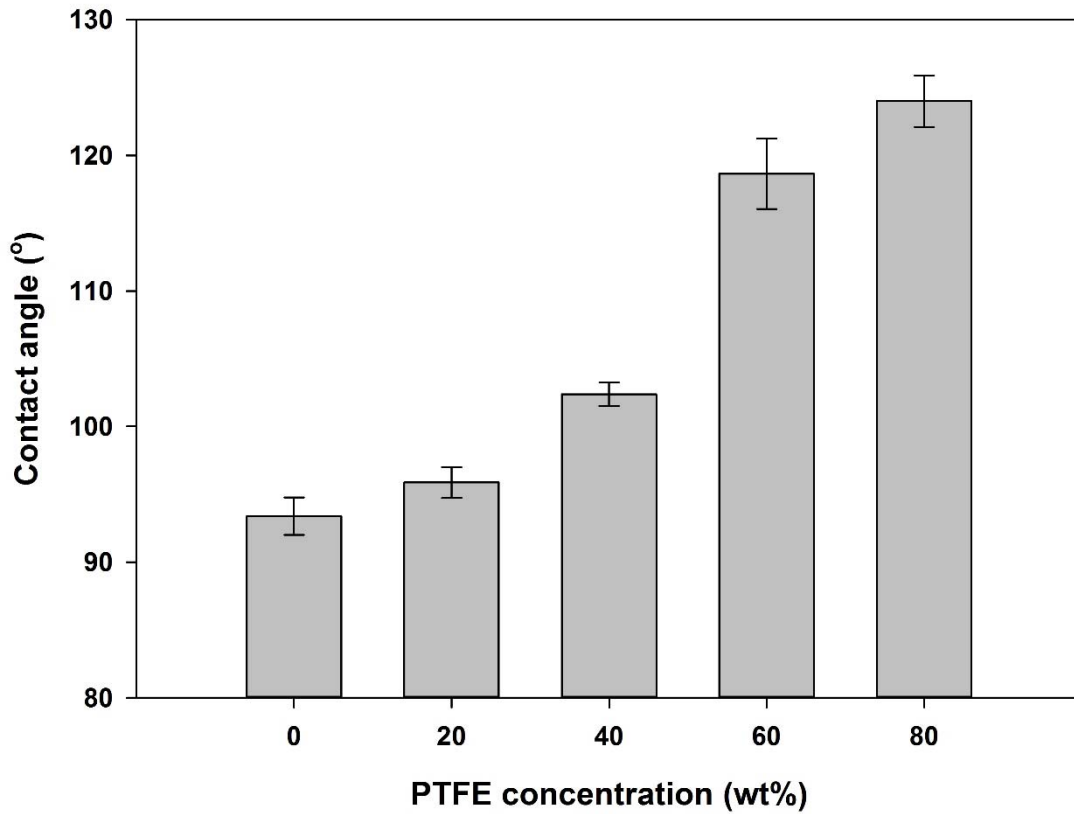


Fig. 17 Comparison of contact angle with different PTFE concentration.

The solution was made to determine the viscosity by PTFE concentration and the viscosity was measured. A solution with too low viscosity was not proper for spinning, so a low content of PTFE solution was made to measure the viscosity. As shown in Fig. 18, the viscosity of PVDF-CTFE pure solution decreased with increasing the content of PVDF-CTFE pure solution. When PTFE was mixed up to 30 wt%, the viscosity was too low and the spinning did not work properly, so 10 and 20 wt% were selected and spinning was carried out.

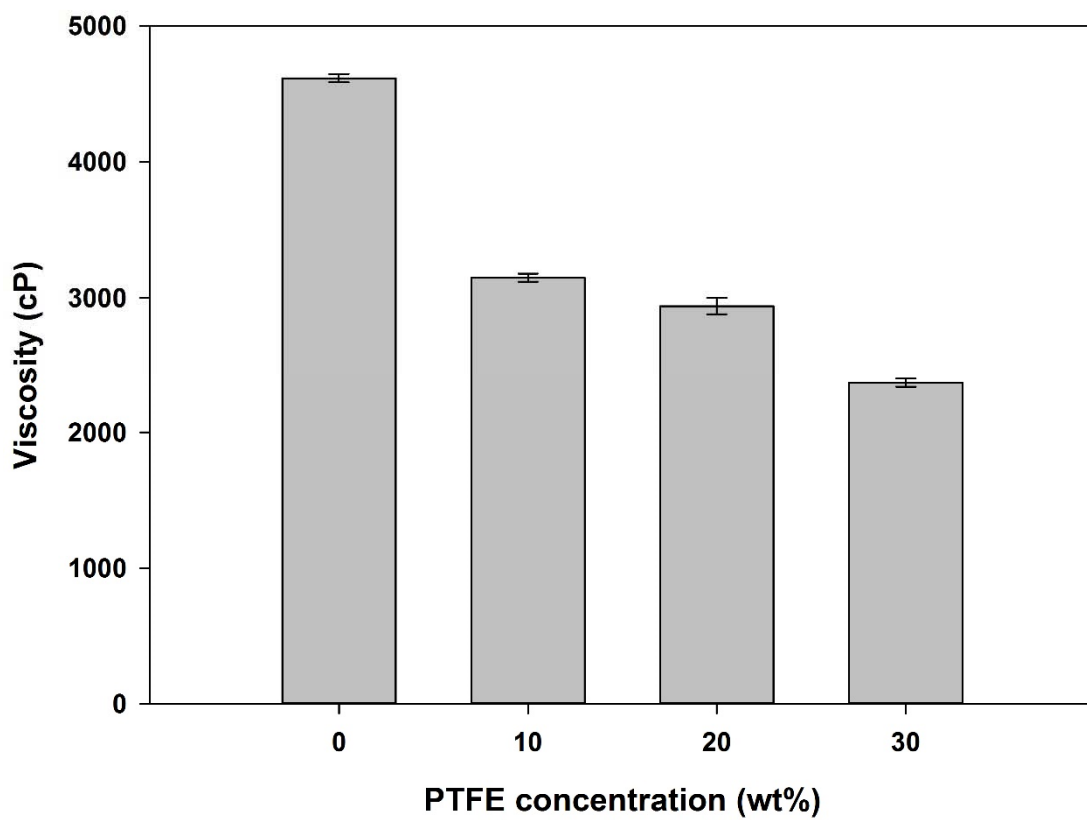


Fig. 18 Viscosity by PTFE concentration.

To observe the effect of PTFE addition, the cross-sectional images of 5, 10, 15, and 20 wt% of the spun hollow fibers are shown in Fig. 19. As shown in Fig. 19, macrovoids are increased with increasing PTFE at 5 and 10 wt%. As a result, it can be seen that the sponge-like structure formed in the center becomes thinner. However, when the content of PTFE is increased to 15 or 20 wt%, it is confirmed that the middle sponge-like structure is formed again and thickened.

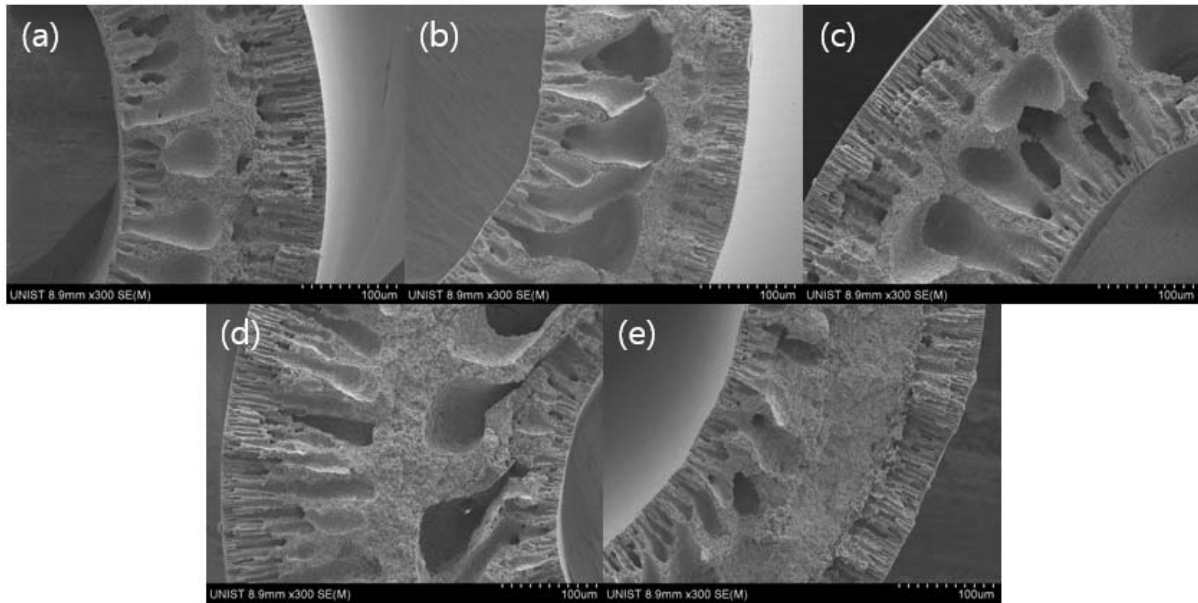


Fig. 19 Comparison hollow fiber's cross-sectional images with different PTFE concentration. (a) Pure dual-layer hollow fiber, (b) Lumen side image for 5 wt% of in inner dope solution, (c) Lumen side image for 10 wt% PTFE in dope solution, (d) Lumen side image for 15 wt% PTFE in dope solution, (e) Lumen side image for 20 wt% PTFE in dope solution.

As shown in Fig. 20, it can be seen that the flux is slightly less than 5 LMH in the case of the dual-layer hollow fiber membrane without adding PTFE. However, when 5 wt% of PTFE is added to the PVDF-CTFE solution, it is confirmed that the flux is larger than 5 LMH as the macrovoids increases as shown in Fig. 19 (b). In addition, it can be confirmed that flux is increased to about 7 after putting 10 wt%. However, it can be seen that the addition of 15 wt% greatly reduces the flux. As shown in Fig. 19 (d), the flux decreases as the sponge-like structure is formed in the center. If PTFE is further added and 20 wt% is added, it can be confirmed that the flux falls to 4 LMH or less. This is due to the thicker intermediate sponge-like structure and can be seen in Fig. 19 (e).

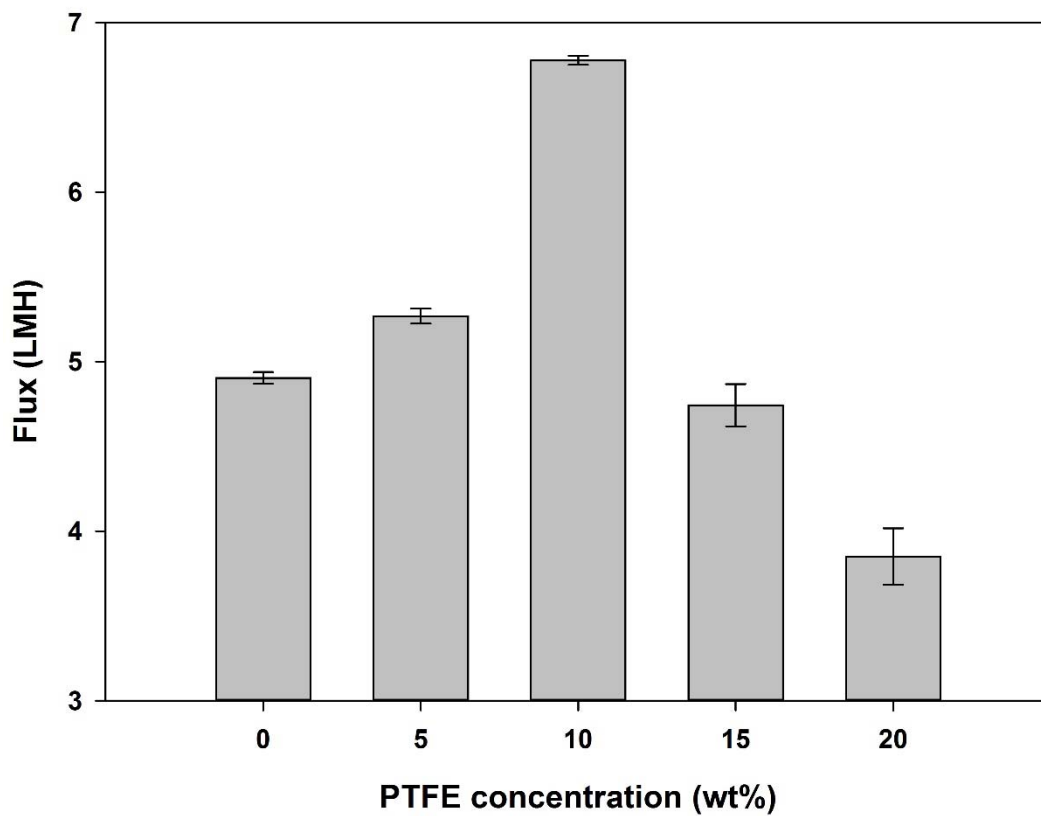


Fig. 20 Comparison of VMD flux change by different PTFE concentration.

Similar to the previous experiment, the LEP experiment was carried out to confirm the hydrophobicity change due to the addition of PTFE. As shown in Fig. 21, it can be seen that the addition of PTFE does not significantly change the LEP. The addition of 5 wt% or 10 wt% of PTFE showed a slight increase in hydrophobicity, but the LEP value did not increase due to the formation of macrovoids inside. Also, after 15 wt%, the middle sponge-like structure started to form again, but the LEP value is not much different from the previous because of the macrovoids inside. However, in the case of 20 wt% PTFE, the inner sponge-like structure is greatly thickened. As shown in Fig. 21, the LEP value is also increased accordingly.

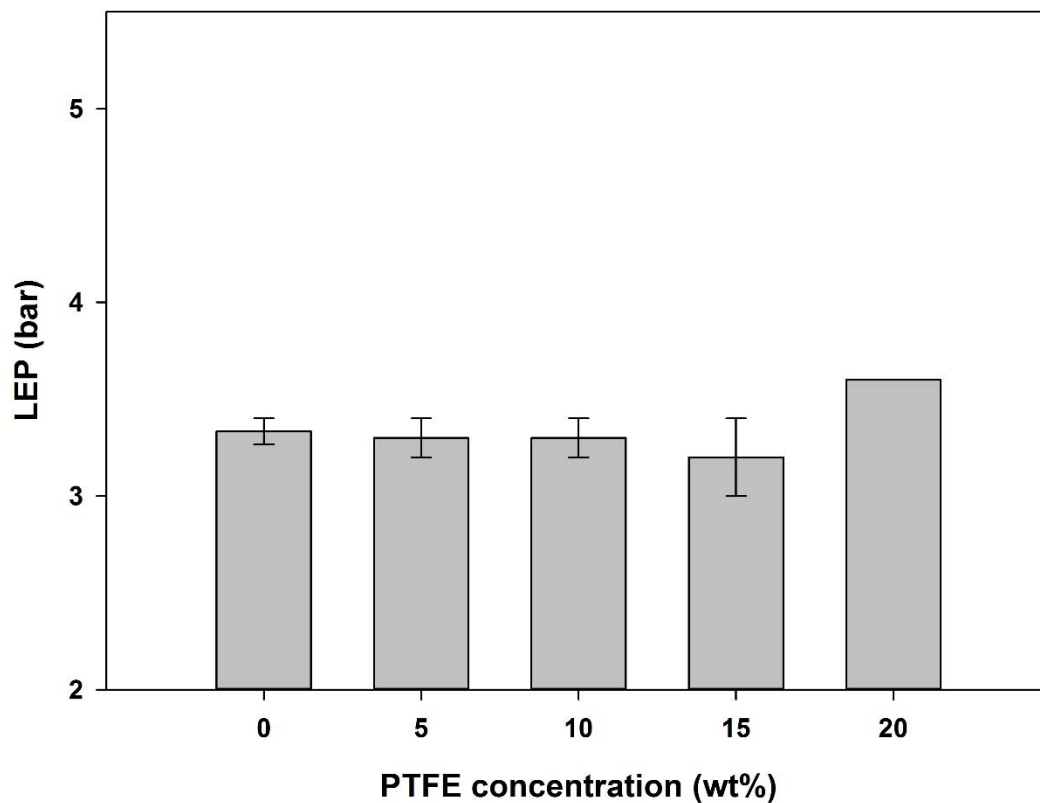


Fig. 21 Change of LEP due to different PTFE concentration.

From the previous experiment, it was confirmed that the structure of the PVDF-CTFE layer changes with the addition of PTFE. It was confirmed that PTFE affects the structure of the hollow fiber as an additive. In addition, it was confirmed that the PTFE had sufficient properties to increase the hydrophobicity. However, it was confirmed that a large amount of PTFE acts as a factor to lower the

viscosity of the solution, thereby causing difficulty in spinning. When 10 wt% of PTFE was added, the macrovoid size of the cross-section was the largest and the flux was also the largest. However, with the addition of PTFE, the sponge-like structure was formed in the middle of the cross-section, and the thickness was thickened and the flux was greatly reduced. The addition of PTFE confirmed the increase in flux due to the structural change, but the contact angle shows that 10 wt% of PTFE does not significantly affect the increase in hydrophobicity. Experiments were carried out through the chemical bonding method as an experiment to increase the hydrophobicity to prevent the wetting phenomenon.

3.2 Improvement of flux of dual-layer hollow fiber membrane through ATRP

As another method for improving the hydrophobicity, ATRP, which is a method for chemical synthesis, can be used. Fluorostyrene was added as a substance to increase the hydrophobicity by removing Cl of the functional group, and the change of the length of branches along the time was observed, and the hydrophobicity was measured by the contact angle.

The modified polymer with fluorostyrene is not dissolved in the solvent when the polymer is directly bonded to the polymer in powder form. Therefore, there is a problem that the hollow fiber can not be formed. Therefore, the hollow fiber of the dual-layer hollow fiber membrane structure is first radiated, and the results were confirmed.

In case of ATRP, twenty dry stranded hollow fibers of 30 cm length are prepared and soaked in ethanol for 24 hours to wet. Then, the reactor is immersed with 200 g of octanol. After that, fluorostyrene, PMDETA, and CuBr are put together and purged with nitrogen for 30 minutes to start the reaction in the absence of air. After purging, the temperature is increased to 80 °C and synthesized until the desired time. After 15, 20, and 25 hours of reaction, remove the hollow fiber from the reactor, immerse it in methanol and wash the remaining chemical for a sufficient time. Subsequently, it is immersed in ethanol for 2 hours, taken out and immersed in hexane for 2 hours, taken out into the air and dried for 24 hours. Fig. 22 shows the result of FTIR measurement of the inside and outside of the hollow fiber to confirm the synthesis result.

In Fig. 22 (a), the inside peak of the dual-layer hollow fiber membrane hollow fiber can be confirmed with time. First of all, PVDF-CTFE has a functional group that can be synthesized with fluorostyrene. As can be seen in the vicinity of 1500 cm^{-1} , it can be seen that peaks which were not observed in pure PVDF-CTFE appear after synthesis. It is a peak of the C=C bond of fluorostyrene, which is shifted on the surface after bonding and shows a peak. It can also be seen that the peak of fluorostyrene increases gradually with time. In the case of Fig. 22 (b), the peak of the PVDF was confirmed by confirming the outside peak of the dual-layer hollow fiber membrane hollow fiber. It can be seen that fluorostyrene did not react with PVDF in the absence of any change compared with the pure PVDF peak over time during the coupling.

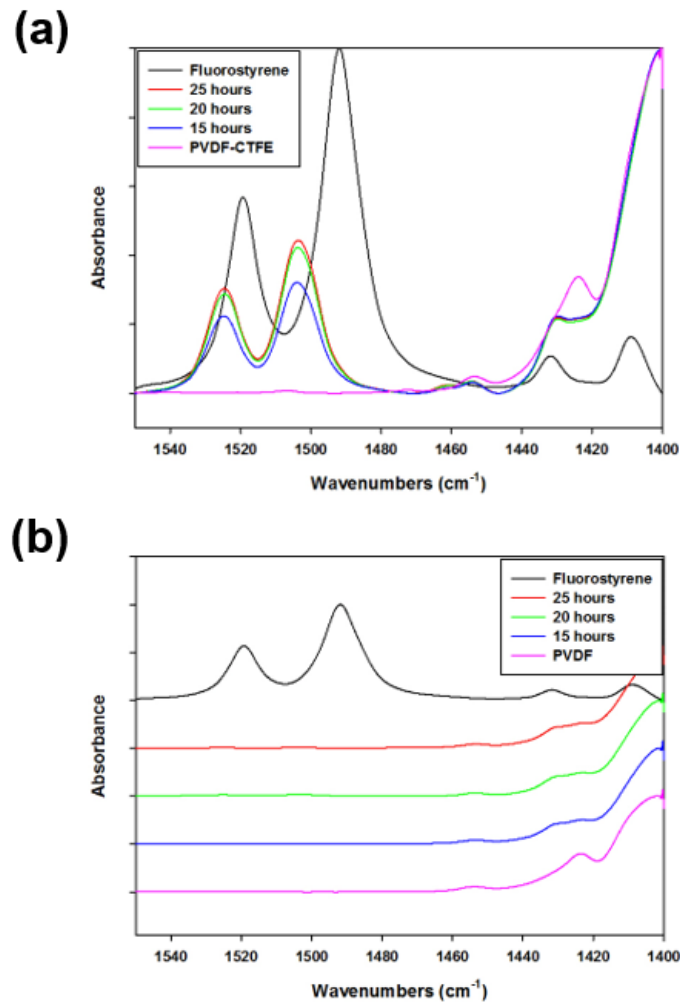


Fig. 22 Comparison of FTIR peaks after ATRP reaction. (a) Change in inner peak of hollow fiber according to ATRP time, (b) Change in outer peak of hollow fiber according to ATRP time.

As shown in Fig. 23, the surface characteristics of XPS can be analyzed. As can be seen in Fig. 23 (a), in the case of C, a new peak of the benzene ring, which was not present on the original surface, appears. Also, the intensity of the peak increases as the synthesis time increases. It can be confirmed that the benzene ring C increased with the synthesis time. In Fig. 23 (b), the peak intensity of Cl is decreased because Cl when the original Cl is separated and pentafluorostyrene is attached due to radical formation. Also, the decrease in peak intensity with time can be confirmed by XPS that Cl is gradually falling off as synthesis progresses like C.

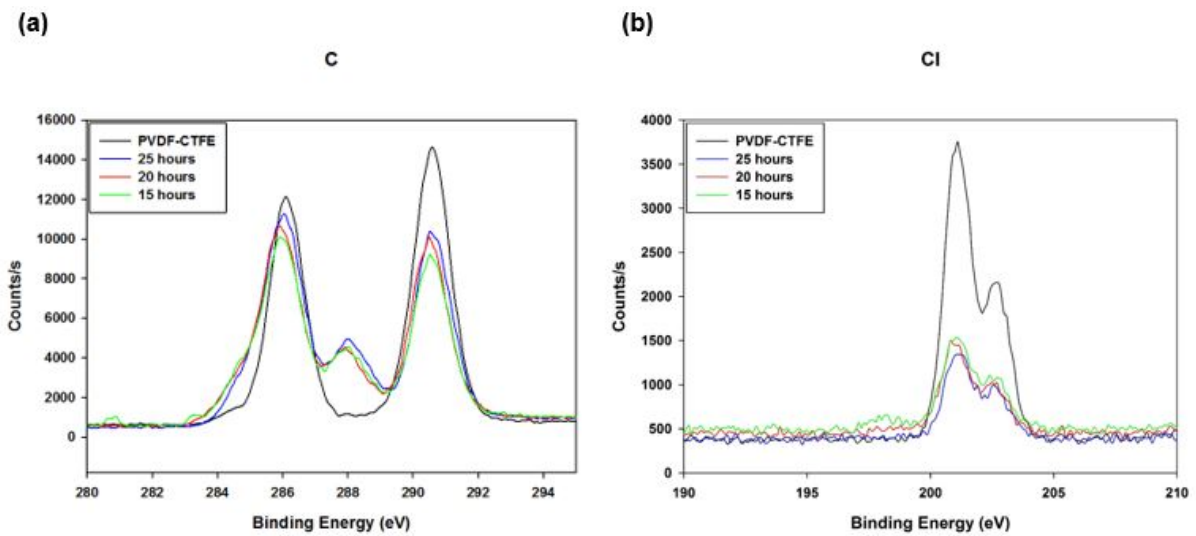


Fig. 23 XPS results following by different ATRP reaction times. (a) XPS C, (b) XPS Cl

Based on the synthesized results, it can be seen that the longer the length of the fluorostyrene branch, since the peak is increased as the synthesis time is increased. In order to confirm that the F-functional group of fluorostyrene is hydrophobic and that the hydrophobicity is increased by attaching to the polymer, a contact angle is confirmed by making a PVDF-CTFE flat membrane. In the case of the flat membrane, a solution of PVDF-CTFE dissolved in 28 wt% of PVDF-CTFE in a DMAc was cast on a glass plate with a supporting knife using a casting knife to a constant thickness of 150 μm . Then, it was placed in an oven maintained at 100 $^{\circ}\text{C}$, and the solvent was blown out for 1 hour to prepare a flat membrane. The contact angle was measured using a prepared flat membrane. The results are shown in Fig. 24. It can be seen that the contact angle increases with time. This indicates that the hydrophobic characteristics of the f functional group of fluorostyrene are increasing with time.

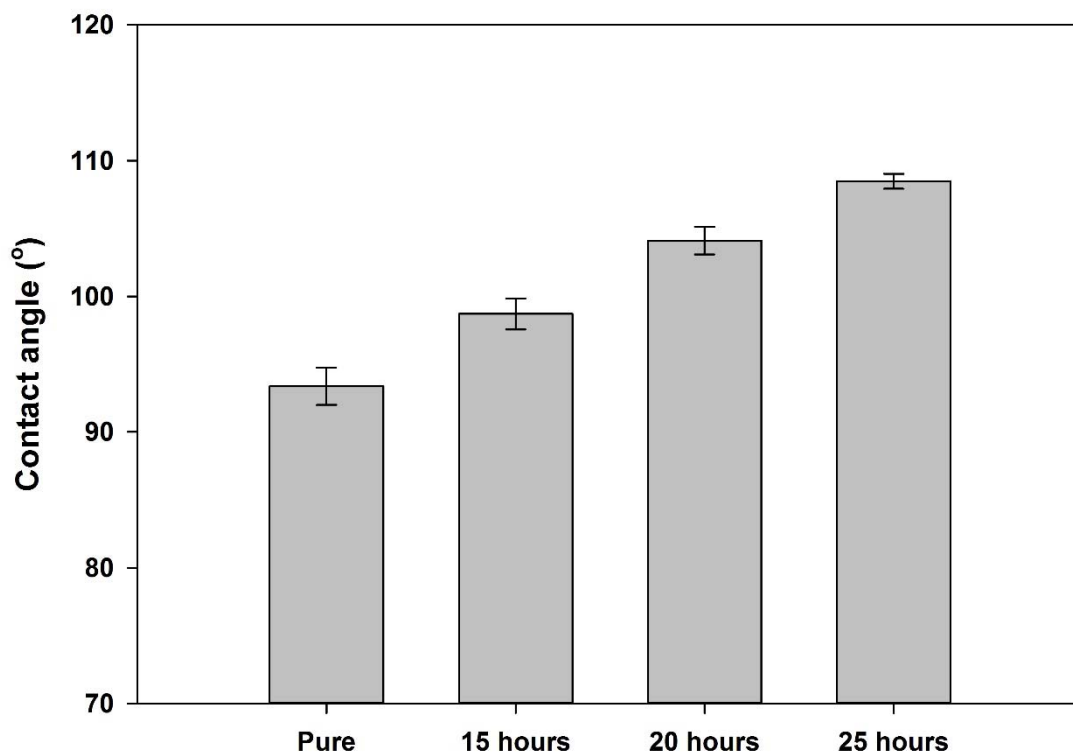


Fig. 24 Comparison of contact angle change with different ATRP synthesis time.

The cross-sectional images of the synthesized hollow fiber prepared by SEM are shown in Fig. 25. It was confirmed by FTIR that the branch of pentafluorostyrene adhered to the PVDF-CTFE layer on the inner side through the chemical synthesis over time, but it can be confirmed that there is no significant change in the thickness of the hollow fiber itself as shown in Fig. 25.

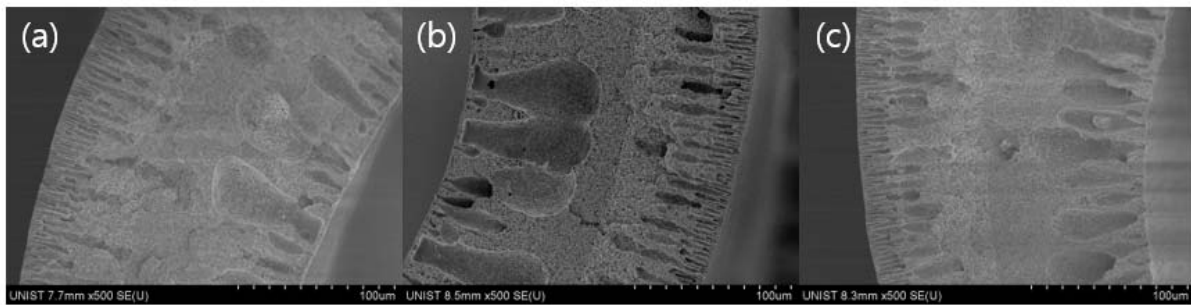


Fig. 25 Cross-sectional images after ATRP. (a) 15 hours ATRP reaction, (b) 20 hours ATRP reaction, (c) 25 hours ATRP reaction.

Fig. 24 shows that the contact angle increases with the synthesis time. As shown in Fig. 25, the pore was not changed much in the cross-sectional image because the modification of the modification through chemical synthesis was performed. Based on these results, performance experiments were conducted through VMD. As shown in Fig. 26, the flux does not increase even contact angle value increased as shown in Fig. 24.

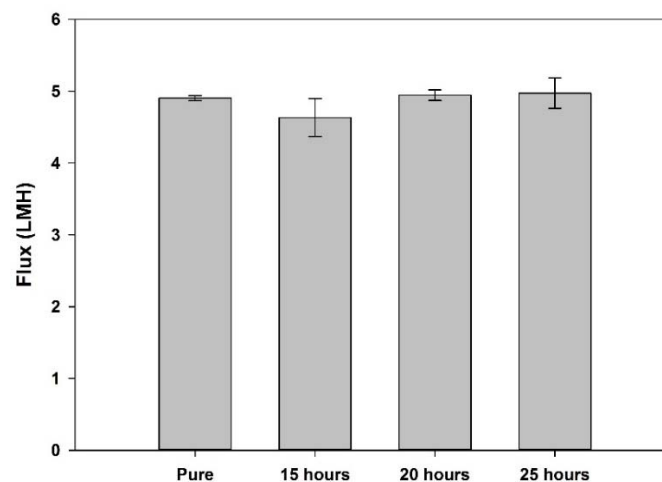


Fig. 26 Comparison of flux according to different reaction time.

Based on these results, LEP experiment was conducted to confirm the prevention of wetting phenomenon due to increasing in hydrophobicity. Hollow fiber was prepared at 20 cm, and the module was fabricated with 5 strands. When 3.5 wt% NaCl solution was pushed to the pore, the pressure was measured until the pore was wetted and the solution was directly passed. This is an experiment that confirms the effect of the hydrophobicity of the membrane on the wetting phenomenon and can be used as an index to confirm the effect of hydrophobicity on the long term experiment.

As shown in Fig. 27, it can be seen that the LEP value tends to increase as the hydrophobicity increases. In the case of the unmodified dual-layer hollow fiber, the LEP increased to 5.1 bars as the contact angle increased by 15° after 25 hours of synthesis, compared to the value of 3.3 bars.

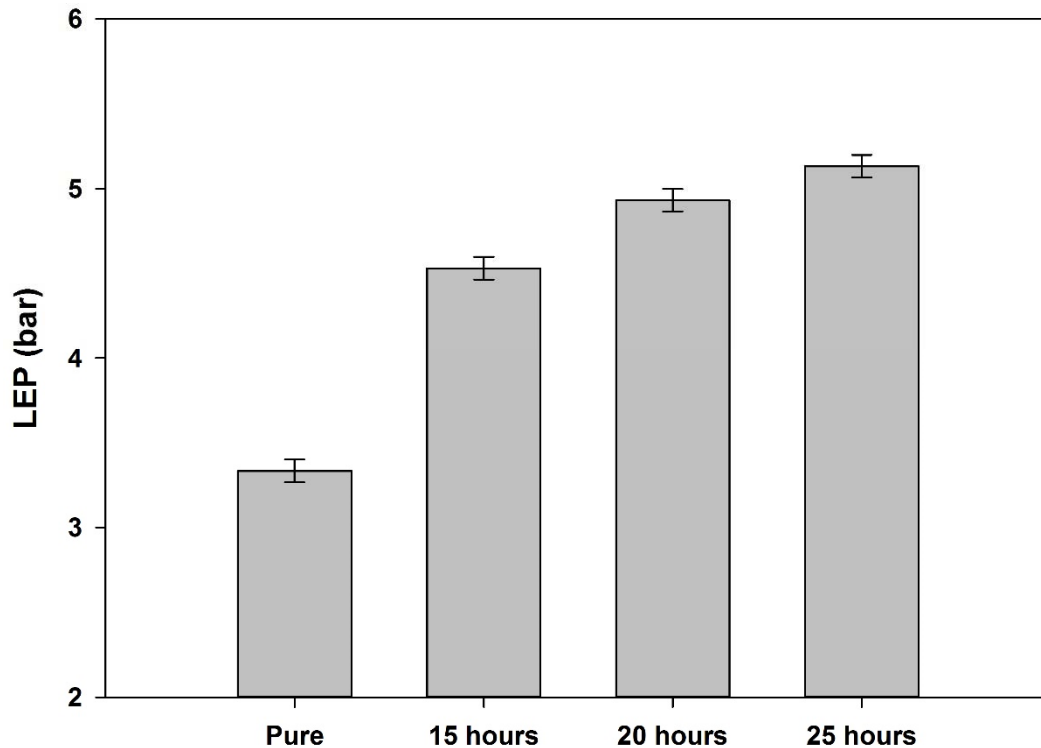


Fig. 27 LEP change with synthesis time.

In the previous experiment, an experiment to increase the hydrophobicity through ATRP was carried out. The hydrophobicity of pentafluorostyrene increased after the synthesis due to the benzene structure and hydrophobic functional group F. The degree of hydrophobicity increased with the synthesis time. The increase of hydrophobicity did not affect the performance of VMD, but it was confirmed that LEP could prevent wetting phenomenon.

VI. Fabricate dual-layer hollow fibers with combined chemical and physical methods

4.1 VMD performance test through LEP and flux measurement

PVDF-CTFE, which has higher hydrophobicity than PVDF, was selected. It has higher flux and hydrophobicity than PVDF but has a large macrovoids formation and weak mechanical strength. To secure this, TIPs method and dual-layer structure were applied to increase mechanical strength. In the case of TIPs, the mechanical strength was improved, but it was confirmed that the flux was significantly lowered, and it was judged that it was not suitable. It was confirmed that the mechanical strength of the dual-layer structure film was increased to a level similar to that of PVDF. However, it was confirmed that the LEP value was lower than that of PVDF, and the physical mixing method and the chemical bonding method were carried out to increase the hydrophobicity. As a physical mixing method, PTFE was used as an additive to confirm hydrophobicity increase and structural change. Although the hydrophobicity was confirmed to increase, the addition of PTFE at a high concentration lowered the viscosity of the solution, and the film formation was proceeded with the addition of a limited concentration. Also, it was confirmed that the flux was increased due to the formation of macrovoids with the addition of PTFE, but LEP was decreased. In the chemical method, the ATRP method was used in which fluorostyrene was dropped on the Cl functional group of PVDF-CTFE. There was no structural change and hydrophobicity was increased, and LEP was increased.

As a method to increase the flux based on the previous experiment, a dual-layer hollow fiber was prepared by adding 10 wt% of PTFE. The hollow fiber was bonded with pentafluorostyrene via ATRP method to increase hydrophobicity and prevent wetting phenomenon. To confirm the results of using both physical and chemical methods, we can confirm that chemical bonding and physical mixing are proceeding properly through FTIR in Fig. 28. As shown in Fig. 28 (a), it can be seen that when PTFE is mixed, there is a peak not present in PVDF-CTFE near 620 cm^{-1} . This is the result of confirming that PTFE is properly mixed. Also, it can be seen that C=C peak of benzene rings appears near 1500 cm^{-1} due to the bonding of pentafluorostyrene. As with the previous results, you can see that it is slightly shifted to the left. From these results, it can be confirmed that PTFE is mixed well inside the hollow fiber and pentafluorostyrene is bonded properly. Fig. 28 (b) shows that pentafluorostyrene was not synthesized in the PVDF on the outside of the hollow fiber.

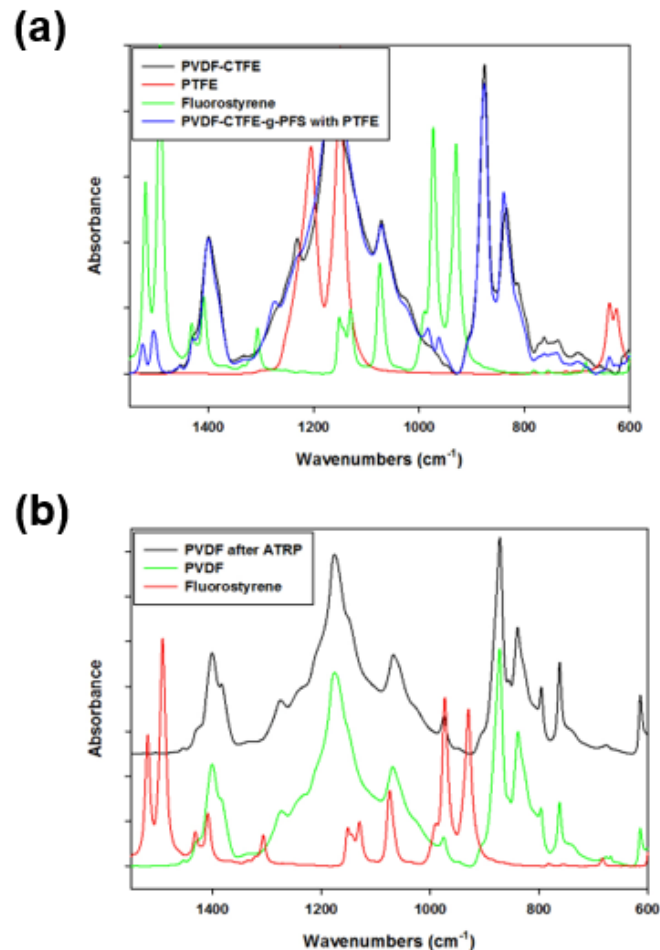


Fig. 28 FTIR peak result after blending and grafting method. (a) PVDF-CTFE-g-PFS synthesis 25 hours which add PTFE 10 wt% before spinning, (b) Outside surface of modified hollow fiber membrane.

As can be seen in Fig. 29, it can be seen that when the ATRP for 25 hours was applied to the hollow fiber mixed with PTFE, there was no change in pore size. This is the same result as the previous ATRP experiment.

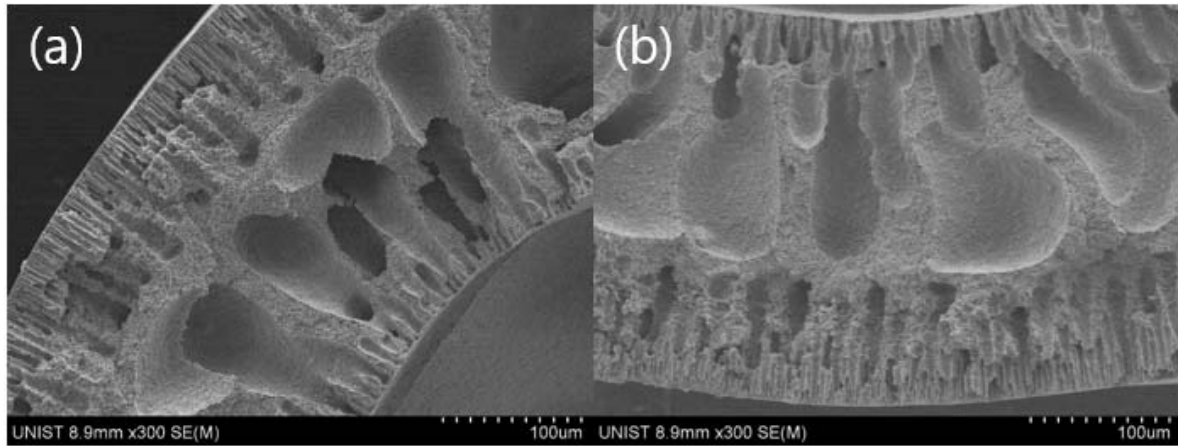


Fig. 29 Cross-sectional images of modified hollow fiber with combined physical and chemical modification method. (a) Dual-layer hollow fiber with PTFE 10 wt%, (b) Dual-layer hollow fiber with PTFE 10 wt% after 25 hours ATRP.

Experiments with VMD were conducted to evaluate the hollow fibers combined with chemical and physical mixing methods. As shown in Fig. 30, the mixing of PTFE significantly improves the flux, which is similar to the case of mixing only PTFE before ATRP. As with the previous results, it can be seen that there is no significant difference in the performance of the VMD that ATRP increases the hydrophobicity.

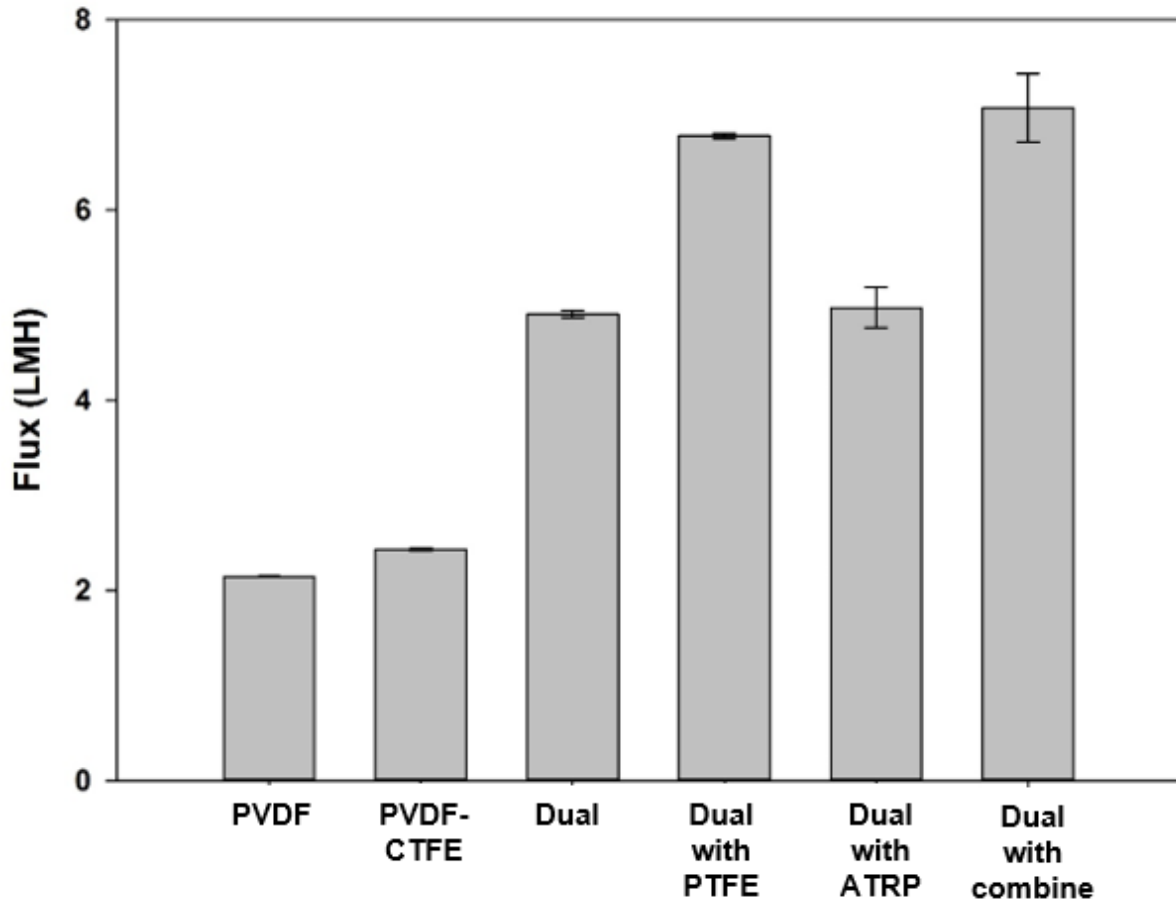


Fig. 30 Comparison of VMD flux with single, dual-layer, modified dual-layer hollow fiber membranes.

LEP experiments were conducted to confirm the increase in hydrophobicity. As shown in Fig. 31, it can be seen that combined dual-layer hollow fiber has lower LEP value than that of the single-layer hollow fiber with 25 hours ATRP but higher than 10 wt% of PTFE in inner dope solution. Because of the macrovoids at lumen side of the hollow fiber caused by PTFE affect LEP but after ATRP, it can be seen that hydrophobicity increased.

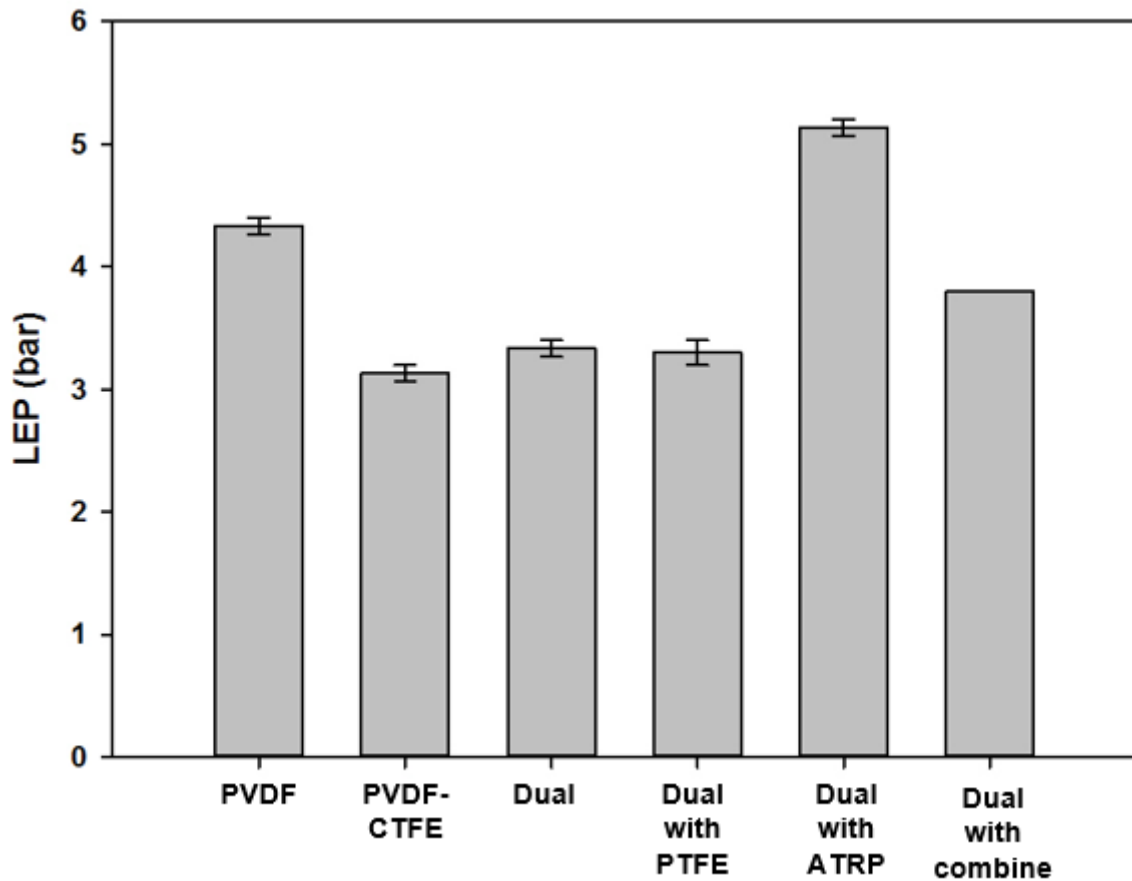


Fig. 31 LEP comparison of LEP with single, dual-layer, modified dual-layer hollow fiber membranes.

Previous experiments have shown successful results in increasing flux through PTFE and increasing hydrophobicity through ATRP. It was confirmed that the cross-sectional structure of the hollow fiber was changed by the addition of PTFE. It was confirmed that the formation of macrovoids did not significantly increase the LEP value despite increased hydrophobicity. To secure this, pentafluorostyrene was bonded to the polymer by a chemical bonding method, and the hydrophobicity was increased to confirm that the LEP value was increased.

As an important factor for preventing the wetting phenomenon, the chemical bonding, and the physical mixing method were carried out for the purpose of increasing the hydrophobicity. It was confirmed that the addition of PTFE as an additive increases the hydrophobicity, but the LEP value did not increase significantly due to the structural change. However, it has been confirmed that hydrophobic properties of hollow fiber are increased by chemical bonding which does not cause structural change and increase hydrophobicity and that LEP also increases with increasing hydrophobicity. It was confirmed that the hollow fiber obtained by the combined method of both methods showed a remarkable increase in both the flux and the wettability when compared with the preceding single hollow fiber.

4.2 Wetting experiment through DCMD

LEP were conducted to confirm the prevention of wetting. In addition, in order to confirm the degree of wetting of membrane in actual MD application, MD experiment was carried out. In the case of VMD, there was no way to check the degree of wetting of the membrane because of direct evaporation due to vacuum. However, in the case of DCMD, the conductivity of the permeate can be measured directly and the degree of wetting can be confirmed. As shown in Fig. 32, in the case of PVDF, the time taken until the conductivity of the permeate becomes 0.01% of the feed is the longest. PVDF-CTFE has a higher contact angle value than PVDF, but it has a macro-void so that takes short time similar to low LEP value. It can also be seen that wetting time is much shorter when 10 wt% of PTFE is blended. This is because the macro-void becomes larger due to the addition of PTFE. For dual-layer membranes, it took longer time until reach 0.01% of feed conductivity than PVDF-CTFE, which, like LEP, because of thickness. As a result of increasing the hydrophobicity through ATRP, it can be confirmed that the membranes reacted for 25 hr took longer than the other dual membranes. However, it can be seen that it gets wet in much less time than PVDF. It can be confirmed that the size of the pore influences the wetting of the membrane as well as the hydrophobicity.

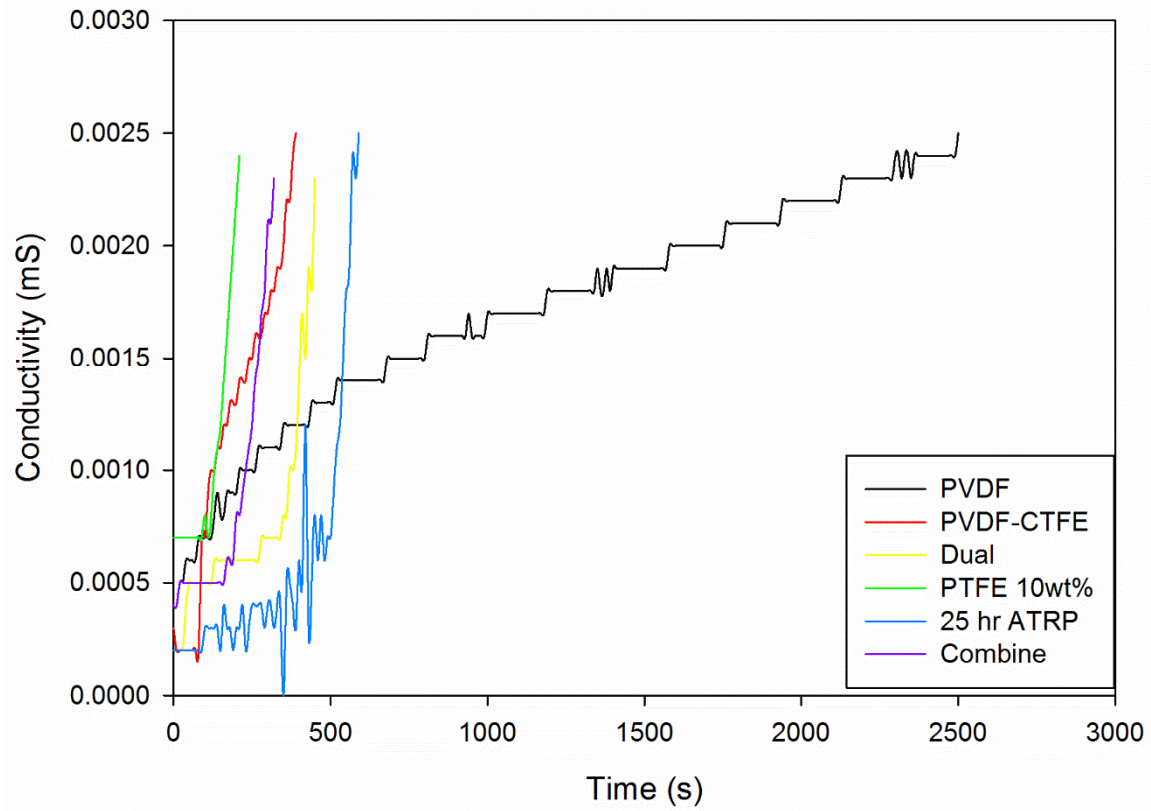


Fig. 32 Comparison of wetting time through DCMD.

Chapter 5. Conclusions

This experiment was conducted to prevent the phenomenon of wetting which is a problem in the membrane distillation method. Experiments were conducted to compare the PVDF-CTFE polymer, which is a widely used polymer, with the polymer PVDF-CTFE, which is not widely used.

PVDF-CTFE has higher hydrophobicity and higher flux than PVDF. However, it was confirmed that it had a problem of the single-layer due to low strength. For solving low mechanical strength, two methods were used. It has been confirmed that the method of spinning the solution at a high concentration through the TIPS method has a high mechanical strength but a low flux. In the case of the dual-layer hollow fiber membrane spinning with PVDF flowing out, the mechanical strength is increased, the middle sponge-like structure disappears, and the flux is also improved.

To further increase the hydrophobicity of the polymer and prevent the wetting phenomenon, the experiment was conducted using two methods. The experiment was conducted as a method of mixing PTFE, which is a substance having higher hydrophobicity characteristics, in a solution for spinning. It was confirmed that the addition of PTFE increased the macrovoids. However, as 15 wt% or more PTFE was added, it was confirmed that the macrovoids became smaller and the middle sponge-like structure became thicker. As a result, the flux also increased from 10 wt% to 15 wt%. The hydrophobicity of pentafluorostyrene with high hydrophobicity was increased by ATRP by chemical method. It was confirmed that the synthesis with PVDF-CTFE was successful and the hydrophobicity was increased by the contact angle. However, it was confirmed that the flux improvement through membrane distillation was not achieved.

In this study, PVDF-CTFE, a polymer that is not used frequently, was spun to be used for membrane distillation and the experiment was conducted in comparison with PVDF. To solve the weak mechanical strength, spinning with dual-layer membrane and TIPS method were carried out. However, TIPS method can increase mechanical strength but severely decrease VMD flux so the TIPS method cannot use for MD in this study. After solving the mechanical strength problem, to further increase hydrophobicity, the physical mixing of PTFE and chemical bonding of pentafluorostyrene were carried out. When PTFE concentration increased in inner dope solution, macrovoids at lumen side was larger until 10 wt% of PTFE. After 15 wt% of PTFE, sponge-like structure generated and got thicker, so that decreased flux. Another increasing hydrophobicity method, ATRP method was conducted. Increasing reaction time, there were changes of FTIR, XPS, contact angle, and LEP value which indicate that hydrophobicity was increased with reaction time. Finally, fabricate dual-layer hollow fibers with optimized PTFE concentration and 25 hours reaction time. Combined dual-layer hollow fiber has higher flux and LEP value than single-layer or dual-layer hollow fiber. Flux increased until 7 LMH which is the higher value

than two single-layer hollow fibers and pure dual-layer hollow fiber and LEP increased until 3.5 bars which is higher than PVDF-CTFE single and dual-layer hollow fiber. However, after blending 10 wt% of PTFE and react with pentafluorostyrene for 25 hours, LEP is not higher than PVDF single-layer hollow fiber. Also, through DCMD experiment, PVDF has longest time until wetting. Even though dual-layer membrane after blending and grafting method has high LEP value, but it took shorter time than pure dual-layer membrane which means that hydrophobicity and pore size affect on membrane's long term property at the same time. Until now, increasing hydrophobicity for preventing wetting phenomenon on MD system. For increasing hydrophobicity, blending and grafting method were used but pore size changed though blending method and this also affect on membrane wetting even though can increase flux. So, further study for preventing wetting phenomenon should be needed.

Reference

1997. *Comprehensive Assessment of the Freshwater Resources of the World*, World Meteorological Organization.
- ALAWADHI, A. A. Regional Report on Desalination GCC Countries. IDA World Congress on Desalination and Water Reuse, March 8-13 2002 Manama, Bahrain.
- ALKHUDHIRI, A., DARWISH, N. & HILAL, N. 2012. Membrane distillation: A comprehensive review. *Desalination*, 287, 2-18.
- APTEL, P., ABIDINE, N., IVALDI, F. & LAFAILLE, J. P. 1985. Polysulfone hollow fibers — effect of spinning conditions on ultrafiltration properties. *Journal of Membrane Science*, 22, 199-215.
- BASINI, L., D'ANGELO, G., GOBBI, M., SARTI, G. C. & GOSTOLI, C. 1987. A desalination process through sweeping gas membrane distillation. *Desalination*, 64, 245-257.
- BECH, L., ELZEIN, T., MEYLHEUC, T., PONCHE, A., BROGLY, M., LEPOITTEVIN, B. & ROGER, P. 2009. Atom transfer radical polymerization of styrene from different poly(ethylene terephthalate) surfaces: Films, fibers and fabrics. *European Polymer Journal*, 45, 246-255.
- BODELL, B. R. 1963. *Silicone rubber vapor diffusion in saline water distillation*. United States patent application.
- BONYADI, S. & CHUNG, T.-S. 2009. Highly porous and macrovoid-free PVDF hollow fiber membranes for membrane distillation by a solvent-dope solution co-extrusion approach. *Journal of Membrane Science*, 331, 66-74.
- BROUSSE, C., CHAPURLAT, R. & QUENTIN, J. P. 1976. New membranes for reverse osmosis I. Characteristics of the base polymer: sulphonated polysulphones. *Desalination*, 18, 137-153.
- CABASSO, I., KLEIN, E. & SMITH, J. K. 1976. Polysulfone hollow fibers. I. Spinning and properties. *Journal of Applied Polymer Science*, 20, 2377-2394.
- CADOTTE, J. E. 1981. Interfacially synthesized reverse osmosis membrane. Google Patents.
- CADOTTE, J. E. 1985. Evolution of Composite Reverse Osmosis Membranes. *Materials Science of Synthetic Membranes*. American Chemical Society.
- CARLSSON, L. 1983. The New Generation in Sea Water Desalination SU Membrane Distillation System. *Desalination*, 45, 221-222.
- CHA, B. J. & YANG, J. M. 2007. Preparation of poly(vinylidene fluoride) hollow fiber membranes for microfiltration using modified TIPS process. *Journal of Membrane Science*, 291, 191-198.
- CHIANG, C.-Y., JAIPAL REDDY, M. & CHU, P. P. 2004. Nano-tube TiO₂ composite PVdF/LiPF₆ solid membranes. *Solid State Ionics*, 175, 631-635.
- CHUNG, T.-S., QIN, J.-J. & GU, J. 2001. Erratum to 'Effect of shear rate within the spinneret on morphology, separation performance and mechanical properties of ultrafiltration polyethersulfone hollow fiber membranes': [Chemical Engineering Science 55 (2000) 1077–1091]. *Chemical Engineering Science*, 56, 5869.
- CREDALI, L., BARUZZI, G. & GUIDOTTI, V. 1978. Reverse osmosis anisotropic membranes based on

- polypiperazine amides. Google Patents.
- DING, Z., MA, R. & FANE, A. G. 2003. A new model for mass transfer in direct contact membrane distillation. *Desalination*, 151, 217-227.
- EDGAR, K. J., BUCHANAN, C. M., DEBENHAM, J. S., RUNDQUIST, P. A., SEILER, B. D., SHELTON, M. C. & TINDALL, D. 2001. Advances in cellulose ester performance and application. *Progress in Polymer Science*, 26, 1605-1688.
- FINDLEY, M. E. 1967. Vaporization through Porous Membranes. *Industrial & Engineering Chemistry Process Design and Development*, 6, 226-230.
- FONTANANOVA, E., JANSEN, J. C., CRISTIANO, A., CURCIO, E. & DRIOLI, E. 2006. Effect of additives in the casting solution on the formation of PVDF membranes. *Desalination*, 192, 190-197.
- FRANCIS, P. S., UNITED, S., NORTH STAR, R. & DEVELOPMENT, I. 1966. *Fabrication and evaluation of new ultrathin reverse osmosis membranes*, Washington, D.C., U.S. Dept. of the Interior; for sale by the Superintendent of Documents, U.S. Govt. Print. Off.
- FRITZMANN, C., L WENBERG, J., WINTGENS, T. & MELIN, T. 2007. State-of-the-art of reverse osmosis desalination. *Desalination*, 216, 1-76.
- GORE, D. W. 1982. Conventional Water Supply Improvement Assoc.
- GRYTA, M. 2007. Influence of polypropylene membrane surface porosity on the performance of membrane distillation process. *Journal of Membrane Science*, 287, 67-78.
- HAN, L-F., XU, Z-L., HAN, L-F., XU, Z-L., YU, L., WEI, Y.-M. & CAO, Y. 2010. Performance of PVDF/Multi-nanoparticles composite hollow fibre ultrafiltration membranes. *Iranian Polymer Journal*, 19, 553-565.
- HOEHN, H. H. & RICHTER, J. W. 1980. Aromatic polyimide, polyester and polyamide separation membranes. Google Patents.
- HOEKSTRA, A. Y. & CHAPAGAIN, A. K. 2008. Frontmatter. *Globalization of Water*. Blackwell Publishing Ltd.
- HOU, D., WANG, J., QU, D., LUAN, Z. & REN, X. 2009. Fabrication and characterization of hydrophobic PVDF hollow fiber membranes for desalination through direct contact membrane distillation. *Separation and Purification Technology*, 69, 78-86.
- J NSSON, A. S., WIMMERSTEDT, R. & HARRYSSON, A. C. 1985. Membrane distillation - a theoretical study of evaporation through microporous membranes. *Desalination*, 56, 237-249.
- JONQUI RES, A., ARNAL-HERAULT, C., BABIN, J., HOEK, E. M. V. & TARABARA, V. V. 2013. Pervaporation. *Encyclopedia of Membrane Science and Technology*. John Wiley & Sons, Inc.
- KHAWAJI, A. D., KUTUBKHANAH, I. K. & WIE, J.-M. 2008. Advances in seawater desalination technologies. *Desalination*, 221, 47-69.
- KHAYET, M. & MATSUURA, T. 2001. Preparation and Characterization of Polyvinylidene Fluoride Membranes for Membrane Distillation. *Industrial & Engineering Chemistry Research*, 40, 5710-5718.
- KUYLENSTIERNA, J., NAJLIS, P. & BJORKLUND, G. 1998. The comprehensive assessment of the

- freshwater resources of the world - Policy options for an integrated sustainable water future. *Water International*, 23, 17-20.
- L.T. ROZELLE, J. E. C., R.D. CORNELIUSSEN, E.E. ERICKSON 1968. Final Report on Development of New Reverse Osmosis Membrane.
- LAWSON, K. W. & LLOYD, D. R. 1997. Membrane distillation. *Journal of Membrane Science*, 124, 1-25.
- M.A. DARWISH, A. D., UNITED ARAB EMIRATES. Desalination Process: A Technical Comparison. IDA World Congress on Desalination and Water Sciences, November 18-24 1995 United Arab Emirates. 149-173.
- MOK, S., WORSFOLD, D. J., FOU DA, A. E., MATSUURA, T., WANG, S. & CHAN, K. 1995. Study on the effect of spinning conditions and surface treatment on the geometry and performance of polymeric hollow-fibre membranes. *Journal of Membrane Science*, 100, 183-192.
- PETERSEN, R. J. 1993. Composite reverse osmosis and nanofiltration membranes. *Journal of Membrane Science*, 83, 81-150.
- PORTER, M. C. 1989. *Handbook of industrial membrane technology*, Park Ridge, NJ (USA); Noyes Publications; None.
- REID, C. E. & BRETON, E. J. 1959. Water and ion flow across cellulosic membranes. *Journal of Applied Polymer Science*, 1, 133-143.
- SARTI, G. C., GOSTOLI, C. & BANDINI, S. 1993. Extraction of organic components from aqueous streams by vacuum membrane distillation. *Journal of Membrane Science*, 80, 21-33.
- SCHNEIDER, K., H LZ, W., WOLLBECK, R. & RIPPERGER, S. 1988. Membranes and modules for transmembrane distillation. *Journal of Membrane Science*, 39, 25-42.
- SCHOFIELD, R. W., FANE, A. G., FELL, C. J. D. & MACOUN, R. 1990. Factors affecting flux in membrane distillation. *Desalination*, 77, 279-294.
- SHAFFER, D. L., ARIAS CHAVEZ, L. H., BEN-SASSON, M., ROMERO-VARGAS CASTRILL N, S., YIP, N. Y. & ELIMELECH, M. 2013. Desalination and Reuse of High-Salinity Shale Gas Produced Water: Drivers, Technologies, and Future Directions. *Environmental Science & Technology*, 47, 9569-9583.
- SHI, J.-L., FANG, L.-F., LI, H., ZHANG, H., ZHU, B.-K. & ZHU, L.-P. 2013. Improved thermal and electrochemical performances of PMMA modified PE separator skeleton prepared via dopamine-initiated ATRP for lithium ion batteries. *Journal of Membrane Science*, 437, 160-168.
- SIRKAR, K. K. 1992. Other new membrane processes. 899-904.
- TEOH, M. M. & CHUNG, T. S. 2009. Membrane distillation with hydrophobic macrovoid-free PVDF-PTFE hollow fiber membranes. *Separation and Purification Technology*, 66, 229-236.
- TEOH, M. M., CHUNG, T. S. & YEO, Y. S. 2011. Dual-layer PVDF/PTFE composite hollow fibers with a thin macrovoid-free selective layer for water production via membrane distillation. *Chemical Engineering Journal*, 171, 684-691.

- TIWARI, G. N., SINGH, H. N. & TRIPATHI, R. 2003. Present status of solar distillation. *Solar Energy*, 75, 367-373.
- TOOMA, M. A., NAJIM, T. S., ALSALHY, Q. F., MARINO, T., CRISCUOLI, A., GIORNO, L. & FIGOLI, A. 2015. Modification of polyvinyl chloride (PVC) membrane for vacuum membrane distillation (VMD) application. *Desalination*, 373, 58-70.
- WEYL, P. K. 1967. Recovery of demineralized water from saline waters. Google Patents.
- YULIWATI, E., ISMAIL, A. F., MATSUURA, T., KASSIM, M. A. & ABDULLAH, M. S. 2011. Effect of modified PVDF hollow fiber submerged ultrafiltration membrane for refinery wastewater treatment. *Desalination*, 283, 214-220.
- YUN, Y., LE-CLECH, P., DONG, G., SUN, D., WANG, Y., QIN, P., CHEN, Z., LI, J. & CHEN, C. 2012. Corrigendum to "Formation kinetics and characterization of polyphthalazinone ether ketone hollow fiber ultrafiltration membranes" [J. Membr. Sci. 389 (2012) 416–423]. *Journal of Membrane Science*, 423–424, 556.
- ZHANG, M. & RUSSELL, T. P. 2006. Graft Copolymers from Poly(vinylidene fluoride-co-chlorotrifluoroethylene) via Atom Transfer Radical Polymerization. *Macromolecules*, 39, 3531-3539.